ANNUAL REVIEWS **Further**

Click here for quick links to Annual Reviews content online, including:

- Other articles in this volume
- Top cited articles
- Top downloaded articles
- Our comprehensive search

Ionophore-Based Optical Sensors

Günter Mistlberger,[1,2] Gastón A. Crespo,[1] and Eric Bakker[1]

[1]Department of Inorganic and Analytical Chemistry, University of Geneva, CH-1211 Geneva 4, Switzerland; email: g.mistlberger@gmail.com, gaston.crespo@unige.ch, eric.bakker@unige.ch

[2]Department of Analytical and Food Chemistry, Graz University of Technology, A-8010 Graz, Austria

Annu. Rev. Anal. Chem. 2014. 7:483–512

The *Annual Review of Analytical Chemistry* is online at anchem.annualreviews.org

This article's doi:
10.1146/annurev-anchem-071213-020307

Copyright © 2014 by Annual Reviews.
All rights reserved

Keywords

ion sensing, pH cross sensitivity, chemical mapping, photoresponsive ion sensors, referenced signals

Abstract

This review provides an overview of the key aspects of designing ionophore-based optical sensors (IBOS). Exact response functions are developed and compared with a simplified, generalized equation. We also provide a brief introduction into less established but promising working principles, namely dynamic response and exhaustive exchange. Absorbance and fluorescence are the main optical readout strategies used in the evaluation of a sensor response, but they usually require a robust referencing technique for real-world applications. Established referencing schemes using IBOS as well as those from other optical sensors are also discussed. Finally, the power of recently developed photoresponsive ion extraction/release systems is outlined and discussed in view of dynamically switchable IBOS or regenerative exhaustive exchange IBOS.

1. INTRODUCTION

IBOS: ionophore-based optical sensors

Optochemical sensors are sensor devices in which an interaction between an analyte and a sensor triggers an optically accessible change in the sensing material. This can be accomplished with an indicator dye that changes its spectral properties (absorbance and/or fluorescence) upon contact with an analyte. A prominent example of such sensors is a pH indicator, where the sample pH influences the protonation degree of the indicator dye and, hence, determines the color of the sensor. Another example is an optical oxygen sensor, where the luminescence intensity and decay time are influenced by the excited-state quenching of an analyte.

When a receptor element does not change its optical properties upon contact with an analyte, an indirect sensing scheme may be used. Here, the binding event of an analyte to a receptor can trigger a secondary, optically detectable process. Ionophore-based optical sensors (IBOS) represent an illustrative example of such sensors. Facilitated by a membrane component (ionophore) with a high affinity toward the analyte, cation sensors, for instance, extract positively charged analytes into the sensing film. In turn, an equivalent amount of protons is released from the sensing phase, thereby changing the protonation degree of the proton carrier (i.e., liphilic pH indicator) (**Figure 1**). The

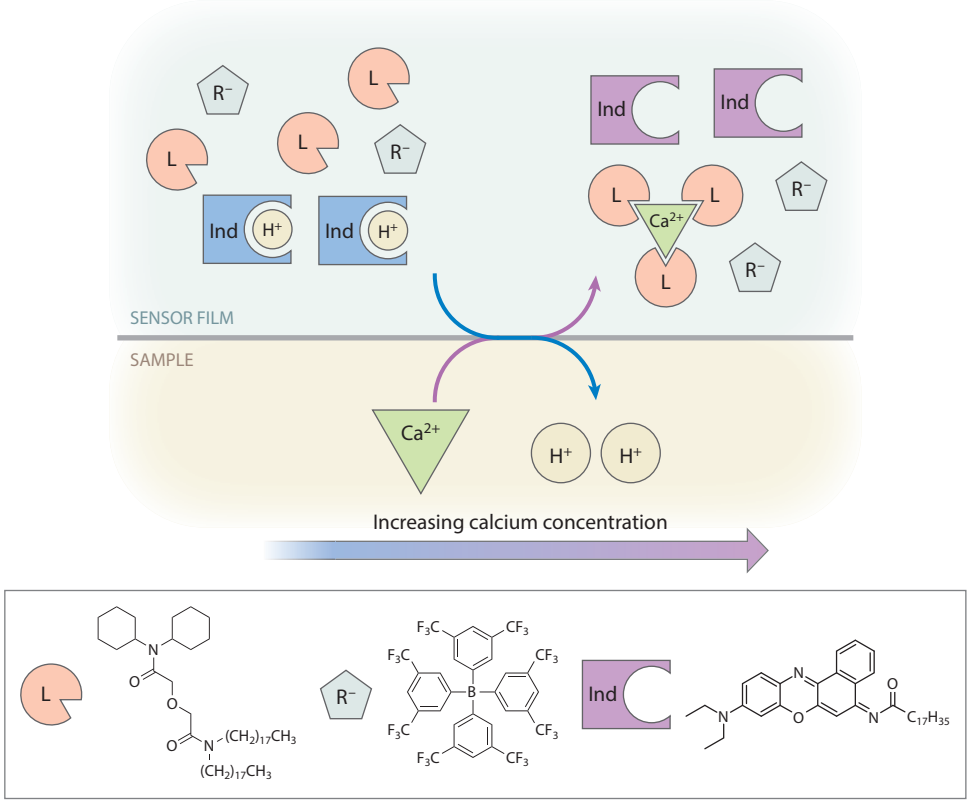

Figure 1

Schematic representation of the ion-exchange process triggered upon increase of the analyte ion concentration, where R^- indicates a negatively charged ion exchanger. Calcium ionophore molecules (L) stabilize the calcium inside the lipophilic liquid/polymeric film (*sensor film*). Electroneutrality is maintained by expelling an equivalent amount of protons, which triggers a detectable change in the color of the reporter dye (Ind).

IONOPHORE AND CHROMOIONOPHORE TERMINOLOGY

Alternative terms for ionophores, such as ligands and carriers, and for lipophilic indicator dyes, such as chromoionophores, are found in the literature. In this review, we use "ionophore" for a molecule that selectively binds to a primary analyte ion. The term "lipophilic pH indicator" is used for a molecule that changes its spectral properties depending on the protonation degree. The widespread term "chromoionophore," literally meaning an ionophore that changes color, is misleading because it does not imply the selectivity for protons, as pH indicator does. Moreover, chromo- or fluoroionophore was also used for ionophores that change their spectral properties with selectivities for ions other than protons. Such ionophores are termed "chromogenic ionophores" if their absorbance spectrum changes and as "fluorogenic ionophores" if their fluorescence emission spectrum changes.

analyte recognition event (ion-ionophore) is thereby translated into a protonation equilibrium, which is more easily accessible to optical readout methods. This review focuses on IBOS, which are based on nonoptically active ionophores and lipophilic pH indicators as transducers for protons, here used as reference ions.

Compared with their electrochemical counterparts, most optochemical sensors share important advantages regarding their applications and sensor formats. Optical sensors are typically easy to miniaturize and cost less to manufacture. They also allow signal readout without physical contact (i.e., remote sensing) and enable researchers using optical imaging techniques to obtain spatially resolved analyte patterns. For IBOS, in particular, ion imaging enables sophisticated microelectrode arrays to be replaced with planar optodes or particle suspensions to achieve two- and three-dimensional analyte concentration maps. Although the latter aspect is considered state of the art for optical oxygen and pH sensors (1–3), very few results have been published using IBOS devices (4). This lack of results can be explained by the availability of water-soluble chromo- or fluorogenic indicators for various ions. As a result, for imaging purposes, the demand for IBOS is less than that for oxygen sensors, where a dissolved indicator approach is impossible. However, ion indicators suffer from modest selectivity and flexibility in terms of their dynamic range. Here, IBOS may be more powerful because investigators can tune their selectivity and even their dynamic range (5) via an optimized combination of ionophores (ligands, carriers) and lipophilic indicator dyes (chromoionophores) (see sidebar, Ionophore and Chromoionophore Terminology). Although scientists have demonstrated the possibility of employing specially synthetized fluoro- or chromogenic ionophores (i.e., lipophilic ion indicators) and discussed their potential advantages, such as low cross sensitivity to pH (6), IBOS that use protons as a reference ion together with an optically silent ionophore are by far more popular. This imbalance may be due to the relative simplicity of designing ion-selective bulk optodes on the basis of the recipe for established ion-selective electrodes. The same ionophores used in ion-selective electrodes can often be combined with a suitable lipophilic pH indicator and, if necessary, an ionic additive. Moreover, because ionophores with different selectivity and affinity toward the analyte may be combined with lipophilic pH indicators that have optimized acidity and spectral properties, IBOS may be optimized for specific purposes. This flexibility has allowed scientists to develop IBOS selective for a wide range of cation- and anion-selective sensors. Physiologically relevant ions, particularly potassium (7–16), sodium (5, 14, 17–22), and chloride (7, 15, 23–31), have been thoroughly investigated. Important ions for environmental and food analysis, such as calcium (7, 15, 17, 21, 32–36), magnesium (37–40), ammonium (20), phosphate (41), carbon dioxide (42), nitrate (29), and nitrite (43, 44), have also been the focus of recent research, especially in view of low-cost and/or disposable IBOS (45–48). Examples for transition metals, such as lead (49–53),

copper (54–56), silver (53, 57–59), mercury (53, 60), uranium (61–63), and cadmium (64) have also been reported. For a comprehensive review of ionophores for all kinds of ionic species and on optodes built using these ionophores, we recommend the excellent review of Bühlmann et al. (65).

IBOS now have a history of more than 25 years. Although a few reports with conceptually similar setups were published in the late 1980s, the field did not grow rapidly until 1990 when Simon and colleagues at ETH Zürich published their first papers based on so-called bulk optodes (28, 66, 67). This term introduced an important property with respect to the IBOS response mechanism: IBOS usually rely on sensing phases where the bulk of the material is in thermodynamic equilibrium with the contacting sample solution, which is in clear contrast to surface optodes where the optically active receptors are in direct contact with the solution. In other words, the response of an IBOS relies on an extraction of the analyte from the sample to the sensor phase, and the activity of the analyte in the sensor phase dictates the sensor signal.

With few exceptions, IBOS are based on the same principle: Selective extraction of the target analyte into a lipophilic liquid membrane introduces either coextraction of an oppositely charged reference ion or release of a reference ion with the same charge. The latter is depicted in **Figure 1**, which shows a calcium-selective IBOS that uses the lipophilic pH indicator ETH 5294 as a reporter dye. In most cases, the reference ions are protons. Accordingly, coextraction is most often found for anion sensors, and ion exchange is more prominent for cation-selective IBOS. Lipophilic ionic sites in the form of ion-exchanger salts are often added to compensate for the charges of the active compounds to obey the charge balance condition inside the sensing phase.

The signal is inherently dependent on the activity ratio between target ions and protons. The resultant cross sensitivity to sample pH often requires additional experimental effort, such as buffering samples during measurement or simultaneous pH measurement with an independent sensor. However, pH dependency can also be exploited to tune the sensitivity toward the target ion (see Section 3.1). In addition, some reports have described different approaches to designing IBOS that are virtually pH independent, such as by using coextraction of a charged solvatochromic dye (68, 69), exploiting potential sensitive dyes (70), or applying fluorogenic ionophores (6).

For carbon dioxide, pH dependency may be avoided via direct sensing of carbon dioxide activity, in contrast to the Severinghaus principle where pH change in aqueous solution is measured upon CO_2 extraction (42). Nonequilibrium-based protocols such as exhaustive extraction can also overcome pH dependency. If a sensor is operated outside of the dynamic range, total extraction of the analyte from a limited volume can be obtained. By analogy to coulometry in electrochemistry, this is an absolute measurement and intrinsically independent of the pH in the sample (see Section 5). The Ames Seralyzer, one of the first commercial devices to employ optical sensors, uses this approach in optical detection of blood components such as potassium (71).

This review focuses mainly on fundamental aspects of bulk IBOS, such as response mechanisms (Section 2), and the theoretical development of the response function, selectivity, detection limit, and response time (Section 3). We also summarize the main conclusions based on these theoretical considerations for sensor design. Although a comprehensive theoretical description of all possible cases is beyond the scope of this review, stepwise development of the most prominent example is provided for interested readers. We then introduce different readout modes (Sections 4.1–4.3) and discuss different signal referencing schemes for IBOS, a necessity for the fabrication of robust optical sensors (Section 4.4). Finally, we introduce photoresponsive ion extraction/release systems as an example of a current development made by our group to the field of IBOS.

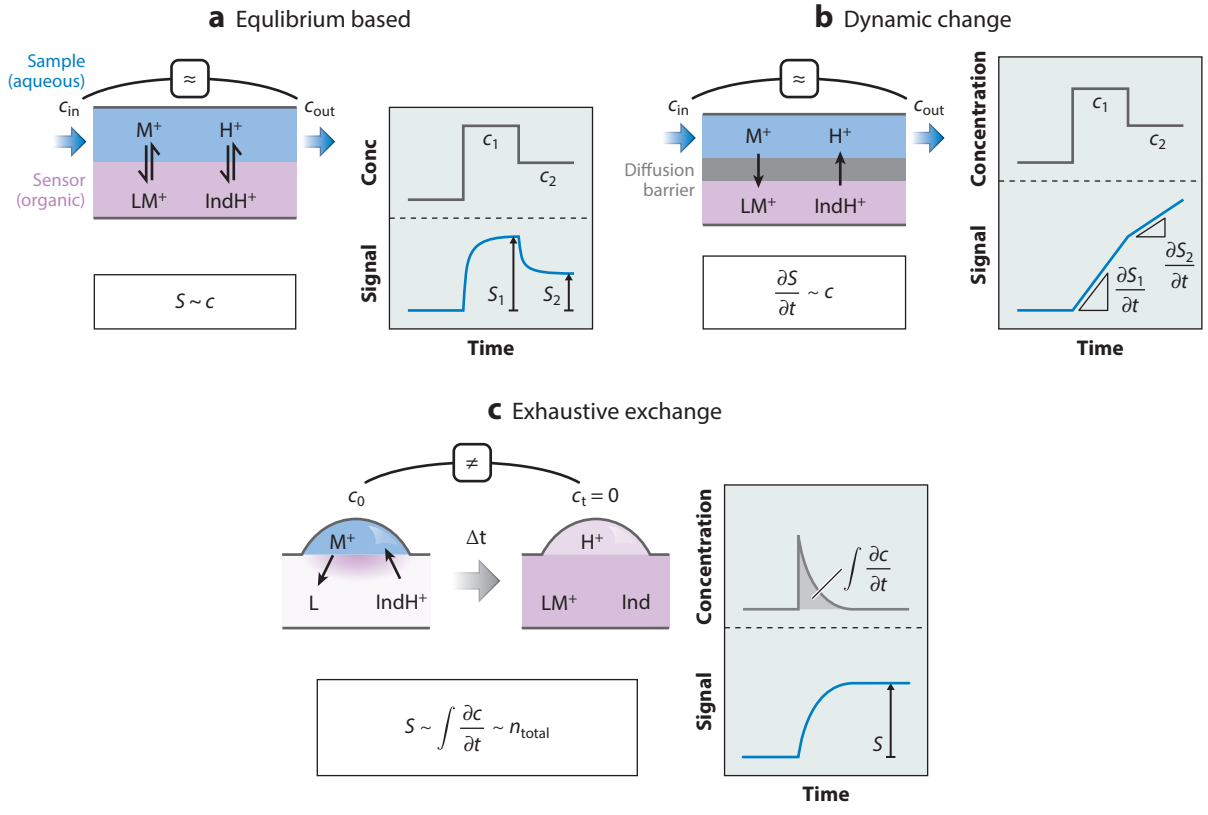

Figure 2

Schematic of three detection principles: (*a*) equilibrium based, (*b*) dynamic change, and (*c*) exhaustive exchange. Equilibrium-based detection principles have been described best and are widely applied, but dynamic change (solution diffusion limited) and exhaustive exchange (absolute measurement) are advantageous in certain situations. Abbreviations: *c*, concentration; Ind, lipophilic pH indicator; L, ionophore; M^+, any cation; *S*, signal.

2. RESPONSE MECHANISMS

2.1. Equilibrium versus Dynamic versus Exhaustive

In equilibrium-based IBOS, the sensor signal is evaluated after complete equilibration of the sensor matrix to the contacting sample phase. All changes in the activity of the primary or reference ion in the sample lead to a new steady-state signal, i.e., a constant protonation degree of the lipophilic pH indicator (**Figure 2*a***). This is similar to other equilibrium-based sensors, such as ion-selective electrodes or solution-phase indicators, with two main differences: First, the readout signal always depends on the activity of two ions simultaneously. Second, in most cases, the necessity for bulk equilibration by ion diffusion inside the matrix material causes longer response times.

In dynamic readout, there is no need to wait for the sensor to be in equilibrium with the sample, because the slope of the sensor response is proportional to the analyte concentration in the contacting solution. This should in theory allow for much faster response times, although this requires a more complex sensor design because the diffusion of analyte to the sensor membrane must be limited to achieve a linear correlation between protonation degree and analyte activity. In **Figure 2*b***, the equilibrium of the target ion is largely on the side of the sensor matrix. In this case,

even a decreasing analyte concentration from c_1 to c_2 triggers an increase of the signal. Ideally, the signal change over time, dS/dt, is proportional to the bulk concentration of the analyte in solution. Because analyte extraction is irreversible, this sensor requires an excess of binding sites to work for a reasonable amount of time. The irreversible nature of such a device is a drawback, as regeneration would require extreme conditions in the contacting solution and/or time-consuming procedures. However, this limitation may be overcome using photoactive compounds (see Section 5). In addition to a potentially faster response time, the dynamic readout also has decreased cross sensitivity to pH. The configuration shown in **Figure 2*b*** uses a diffusion layer to control the analyte mass transport. Thus, the signal change depends chiefly on the gradient across this diffusion layer. In a related approach, the ion-selective lipophilic membrane can be separated from an aqueous detection compartment containing a dissolved fluoro- or chromogenic ionophore. Buffle and coworkers employed this approach by using so-called doped permeation liquid membranes to selectively transport free copper ions toward an aqueous detection compartment (72).

The concept of nonequilibrium operation can also be exploited for exhaustive exchange systems in which the IBOS depletes the analyte ion in the provided sample (**Figure 2*c***). An exhaustive extraction process is followed by a change in indicator signal, which should ideally be directly proportional to the total amount of analyte ions in the sample. A small and defined sample volume is required with an appropriate analyte amount that does not exceed the binding capacity of the sensor. Such a system may be calibration free if the transduction mechanism allows for the determination of the total number of deprotonated indicator molecules. In other cases, a one-time calibration of the signal versus protonated indicator should be sufficient to allow interference-free, absolute analyte detection in defined sample volumes. This approach is very useful for test-strip sensors combined with low-cost, optical readout units. In fact, one of the very first readout devices for optical sensors, the reflectance spectrometer Ames Seralyzer (Miles Laboratories), used this approach to allow for pH-independent ion detection (20). The irreversible nature of exhaustive exchange makes it well suited for disposable sensors. Coupled with photoactivated regeneration, this approach may also find application in reusable sensors.

2.2. How to Make an IBOS Work?

To develop a new sensor, one first has to answer a few questions: What is the charge of the analyte? Which ionophore is available for this analyte, and what is its charge and complexation stoichiometry? Which lipophilic indicator is compatible with my system in terms of readout technology, and what is the charge in its deprotonated state? In **Figure 3**, we provide an overview of various combinations of indicators and ionophores for cations and anions (maximum single charged for ionophores and indicators). In the most prominent case (**Figure 3*e***), a neutral ionophore (L); a positively charged, protonated indicator ($IndH^+$); and a negatively charged ion exchanger (R^-) to maintain electroneutrality are combined to form a cation-selective IBOS. Extraction of a target cation (I^+) into the optode results in the release of a proton, changing the protonation degree and, consequently, the color information of the indicator (**Figure 1**). When the combination of ionophore and indicator has a net neutral charge before the analyte ion enters the sensor phase, an ion exchanger may not be necessary (**Figure 3*b*,*d*,*h*,*j***). In special cases (see **Figure 3*c*,*f*,*i*,*l***), the ionophore also acts as the indicator, meaning that a binding event to the target ion triggers a change in spectral information. Such ionophores are referred to as chromogenic when describing a changing absorption spectrum or as fluorogenic in cases of a changing fluorescence emission spectrum. Depending on the structure, chromogenic ionophores may be able to complex both protons and target cations (**Figure 3*c*,*f***), or the complexation could result in an exchange of a secondary cation bound to anionic sites present in the membrane (not shown). Similar considerations

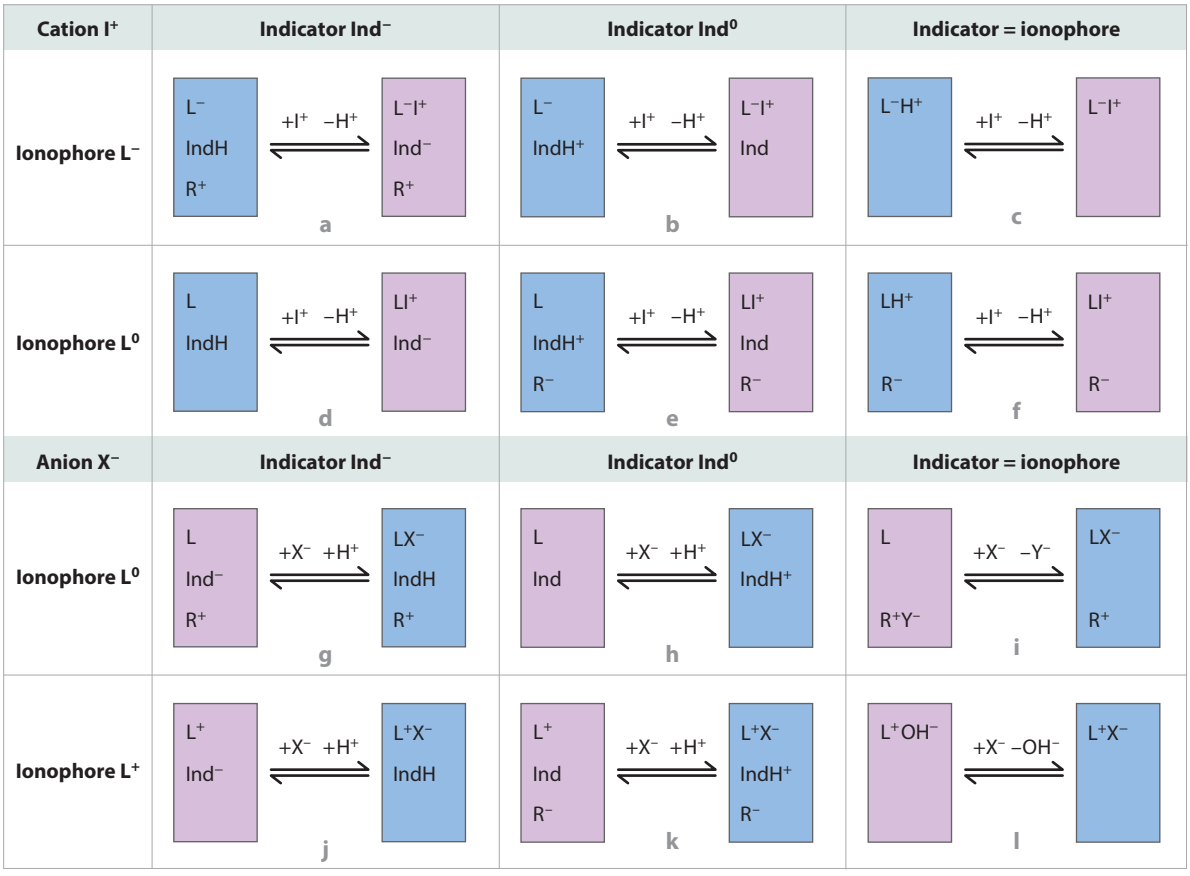

Figure 3

Sensor matrix providing an overview of popular combinations of the following components based on their charge and the nature of the analyte: ionophores (L), lipophilic pH indicators (Ind), and ion exchangers or lipophilic ionic sites (R).

are valid for anions when the target ions are either exchanged with secondary anions stabilized by cationic sites in the membrane (**Figure 3*i***) or with hydroxide ions bound to the chromo/fluorogenic ionophore (**Figure 3*l***). A comprehensive list of all possible combinations found in the literature is beyond the scope of this review.

Figure 1 shows the structures of a prominent example for a calcium ionophore, a lipophilic pH indicator, and a cation exchanger. Calcium ionophores are often based on analogous EDTA binding sites, whereas the most selective sodium ionophores are based on calixarene structures (23). Ionophores for some anions are now available, but performance may still be improved, especially for phosphate and sulfate.

In terms of pH indicator, most IBOS are based on lipophilic Nile blue derivatives. Most of these dyes were originally developed by the Simon lab at ETH Zürich (73) and later commercialized as chromoionophores by Sigma Aldrich. The introduction of long lipophilic chains was necessary to increase solubility in the hydrophobic sensor matrix and thereby suppress leaching of the active compound from the sensor into the sample solution. Most of these dyes carry a single positive charge in their protonated state. Neutral protonated indicators are also described and are usually based on hyrdoxy-azo-compounds (e.g., ETH 2412) or fluorescein derivatives. Using protons as

the reference ion in IBOS is attractive given the high selectivity of available proton ionophores. Complexation with other cations can usually be neglected (73).

The main characteristics of a lipophilic-charged carrier (R) are a permanent charge (positive or negative), a negligible tendency for ion pairing, and no affinity to protons. In other words, an ideal anionic or cationic additive should compensate only for charge imbalances in the membrane without participating in any other complex formation or dissociation processes. Most of these requirements are satisfied by bulky, lipophilic ions, such as tetrakis[3,5-bis(trifluoromethyl)phenyl]borates as anionic sites or tridodecylmethylammonium salts as cationic sites. As shown in **Figure 3**, the necessity of using an anionic or cationic additive does not depend on the charge of the analyte, but rather on the combined charge of ionophore and indicator in the initial state. For a more comprehensive list of available ionophores, indicators, and ionic additives, we refer the reader to other extensive reviews (65, 74).

2.3. Overcoming pH Cross Sensitivity

As a result of an optically silent ionophore and a lipophilic pH indicator as reporter, IBOS have an intrinsic pH cross sensitivity. However, this cannot always be exploited to adjust the responsive range (see Section 3.1). Instead, it often limits the practical applicability of IBOS in real samples. Researchers trying to overcome this pH dependency have devised different solutions, some of which are introduced below. A system based on the coextraction of solvatochromic dyes or the partial exchange of potential sensitive dyes with the analyte ions has been successfully applied for chloride and potassium (68–70). Here, the detection principle is coupled not to the protonation degree of an indicator but rather to the local environment of charged reporter dyes, which depends on the analyte concentration in the contacting sample solution.

In another study, Citterio et al. (6) synthesized a lithium ionophore coupled with a fluorescent reporter. This fluorogenic ionophore showed negligible pH dependence over a wide range from 6 to 8. In general, using fluoro- or chromogenic ionophores is a promising approach to overcome this pH limitation, and a number of such compounds have been reported (75–78). However, not all ionophores in this class are pH independent. Some ionophores, for instance, exchange protons with analyte ions and therefore will show a behavior similar to that of conventional IBOS. Furthermore, chromogenic ionophores based on a photoinduced electron transfer usually depend on pH, at least below a certain threshold (79).

Simultaneous correction for the pH value also results in a virtually pH-independent IBOS. This can be done either by measuring the pH value with a separate sensor or by using a system in which the signal depends on the activity of protons and the target-related species in a reverse way. Xie et al. (42), for instance, demonstrated a pH-independent optical sensor for carbon dioxide in solution or a humidified gas phase. Here, the correlation between pH and the carbonate/carbon dioxide equilibrium was exploited to perform an in situ correction for the pH value to directly detect carbon dioxide.

As mentioned above, the use of IBOS outside of the equilibrium range will also result in virtually pH-independent sensors. If, for instance, the state of the sensor prohibits proton extraction in favor of the extraction of analyte cations, the sensor will absorb ions until either the sensor is saturated or the sample is depleted. If the sensor is far from its equilibrium state, this process should be largely independent of proton activity in the contacting sample solution.

Crespo et al. (80–82) recently introduced an unconventional and exciting alternative for an optical, electrochemiluminescent readout of ion concentrations without the necessity of a reference ion. Here, the potential at the sensing membrane interface was used to modulate the reference potential in a three-electrode cell. A working electrode, responsible for generating electrogenerated

chemiluminescence, was placed in a separated compartment together with a counter electrode (both compartments were bridged). A variation in the activity of the primary analyte (i.e., calcium) provoked a change in the reference potential that directly translates into a different amount of emitted light (electrogenerated chemiluminescence). This approach allows one to accomplish a direct, proton-independent optical readout for IBOS.

3. THEORETICAL DEVELOPMENT OF RESPONSE FUNCTION AND OTHER RELEVANT PARAMETERS

3.1. Response Function for the Target Ion

Developing the response function [signal = f(a_I)] for an IBOS is a crucial step for identifying the influential factors and parameters suitable for tuning the sensor response. We here demonstrate this stepwise process for an ion-exchange system selective for cations of charge z (I^{z+}) that contains a neutral deprotonated pH indicator (Ind^0), an ionophore with complex stoichiometry n (L_nI^{z+}), and an anionic additive (R^-). Other systems as shown in **Figure 3** can be developed by analogy.

The system described here is similar to the combination shown in **Figure 3*e***. As evident from the diagram, the system is based on ion exchange, i.e., extraction of analyte cations into the membrane triggers a release of protons into the sample solution to maintain the charge balance inside the membrane. The target ion starts in the aqueous phase, and the proton begins in the organic phase. After the exchange, their location should be switched. For each cation with charge z, an equivalent amount of z protons needs to be released.

$$z\,H^+(org) + I^{z+}(aq) \rightleftharpoons z\,H^+(aq) + I^{z+}(org). \quad 1.$$

Although charged hydrophilic species exhibit low affinity for a lipophilic polymer matrix, the presence of the lipophilic ion exchanger (charge balance) requires their extraction.[1] Binding the ions to the lipophilic ligands further impacts the overall ion-exchange equilibrium, i.e., a lipophilic pH indicator for protons and an ionophore for target ions. Whereas the stoichiometry between pH indicators and protons is usually 1 to 1, ionophores for cations frequently favor other stoichiometries. Introducing n as the complex stoichiometry between L and I may be used to account for this difference. Thus, the new ion-exchange equilibrium including the stabilized species can be expressed as

$$z\,IndH^+(org) + I^{z+}(aq) + n\,L(org) \rightleftharpoons z\,Ind^0(org) + L_nI^{z+}(org) + z\,H^+(aq). \quad 2.$$

Note that this relationship could also be written by considering the ion exchanger:

$$z\,IndH^+(org) + I^{z+}(aq) + n\,L(org) + z\,R^-(org) \rightleftharpoons z\,Ind^0(org) + L_nI^{z+}(org) + z\,H^+(aq) + z\,R^-(org). \quad 3.$$

The associated overall exchange constant can be formulated as follows:

$$K_{exch}^{IndH^+,L_nI^{z+}} = \frac{[Ind^0]^z(a_H)^z[L_nI^{z+}]}{[IndH^+]^z[L]^n a_I}, \quad 4.$$

where square brackets denote species in the organic phase and free ionic species in the aqueous phase are replaced by their respective activities. Accordingly, the activity for the anionic additive can be eliminated, because R does not participate in any interactions with the ionic species in

[1] When preparing a membrane cocktail, neither pH indicator nor ion exchanging salt have a net charge, but rather exist in their neutral state. Some indicators clearly show this by showing the respective color of the neutral, noncharged state. However, when in contact with a solution of appropriate pH, the indicator dye quickly protonates, thereby triggering a release of the ion exchanger's counter ion into the solution. This process is analogous to membrane conditioning in ion-selective membranes for potentiometry.

the membrane (e.g., ion pairing). Although a valid assumption in most cases, this can severely complicate theoretical description in highly apolar plasticizers such as DOS (83). For the sake of simplicity, we here consider negligible ion pairing.

To establish a correlation between a signal S and ion activity a_I, Equation 4 shows the activity of the target ion in the sample solution. In addition, the signal has to be correlated with the protonation degree of the indicator, which introduces another relationship:

$$1 - \alpha = \frac{[IndH^+]}{Ind_T}, \qquad 5.$$

where Ind_T denotes the total indicator concentration in the optode (known from the membrane preparation). Thus, the concentrations of protonated indicator in the organic phase can be expressed in terms of the protonating degree $1-\alpha$ and the total indicator concentration. The remaining unknowns in the organic phase are the deprotonated indicator $[Ind^0]$, the uncomplexed ionophore concentration $[L]$, and the ionophore-ion-complex concentration $[L_nI^{z+}]$. Mass and charge balances are therefore introduced to replace the unknown parameters. The mass balances are simply given by the fact that the total amount of indicator or ionophore (each known from the optode preparation) is equal to the sum of all compounds containing the species:

$$Ind_T = [IndH^+] + [Ind^0]; \qquad 6.$$

$$L_T = [L] + n[L_nI^{z+}]. \qquad 7.$$

The charge balance originates from the electroneutrality condition in the organic phase. Here, the anionic additive is the only anionic species; therefore, its concentration must be equal to the sum of the positive charges:

$$R_T = [IndH^+] + z[L_nI^{z+}]. \qquad 8.$$

To replace the unknown terms in Equation 4, we find solutions for each species on the basis of known concentrations of $[IndH^+]$ only:

$$\begin{aligned} [L] &= L_T - \frac{n}{z}(R_T - [IndH^+]) \\ [Ind^0] &= Ind_T - [IndH^+] \\ [L_nI^{z+}] &= \frac{R_T - [IndH^+]}{z} \end{aligned} \qquad 9.$$

Then we insert all terms into the exchange constant (Equation 4), replace $[IndH^+]$ with the protonation degree from Equation 5, and solve for the activity of the target ion a_I to obtain the response function:

$$a_I = \frac{1}{zK_{exch}^{IndH^+,L_nI^{z+}}} \left(\frac{a_H\alpha}{1-\alpha}\right)^z \frac{R_T - (1-\alpha)Ind_T}{\{L_T - z^{-1}n[R_T - (1-\alpha)Ind_T]\}^n}. \qquad 10.$$

3.2. Introducing pK_a (Indicator) and the Complex Formation Constant (Ionophore)

To optimize the properties of the different sensor components, one may split the overall exchange constant into the factors that contribute to it. The overall exchange constant already contains expressions similar to the acidity and complex formation constants inside the organic (sensor) phase. The only difference is that the concentrations of the free protons and analyte ions are given for the aqueous phase (a_H and a_I). The concentrations of the species in the organic phase are a

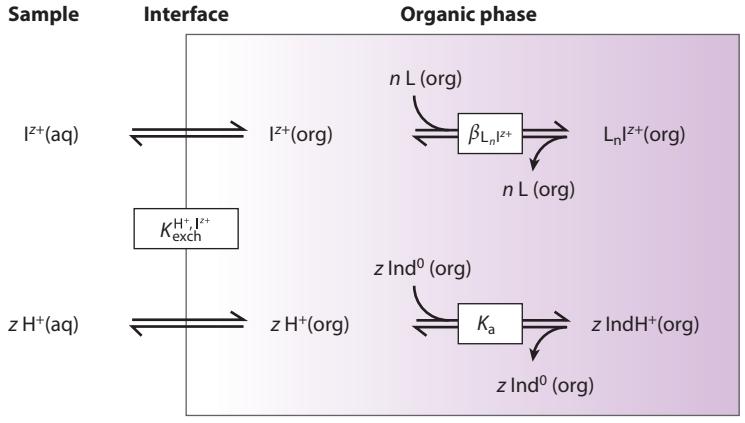

Figure 4

Schematic showing the virtual processes involved in the complexation of analyte ions from a sample with an ionophore. Electroneutrality is retained via ion exchange with an equivalent amount of protons. Abbreviations: aq, aqueous; org, organic.

function of their respective activities in the contacting aqueous solution. In other words, both the primary ion and protons cannot directly form the complex with their ligands. Instead, they first need to be transferred from the aqueous to the organic phase, requiring a transformation from a_I (aq) and a_H (aq) to $[I^{z+}]$ and $[H^+]$, respectively (see **Figure 4**).

The ion-exchange process of the single ions at the interface is expressed with the exchange equilibrium according to Equation 1. The exchange constant for the naked ions $K_{exch}^{H^+,I^{z+}}$ is then given as

$$K_{exch}^{H^+,I^{z+}} = \frac{(a_H)^z[I^{z+}]}{[H^+]^z a_I}. \qquad 11.$$

Now the acidity constant and complex formation constant can be formulated as follows:

$$\begin{aligned} &z\,\mathrm{IndH^+(org)} \overset{K_a}{\rightleftharpoons} z\,\mathrm{Ind(org)} + z\mathrm{H^+(org)} \\ &n\,\mathrm{L(org)} + \mathrm{I^{z+}(org)} \overset{\beta_{L_nI^{z+}}}{\rightleftharpoons} \mathrm{L}_n\mathrm{I^{z+}} \end{aligned} \quad ; \qquad 12.$$

$$\begin{aligned} (K_a)^z &= \frac{[Ind^0]^z[H^+]^z}{[IndH^+]^z} \\ \beta_{L_nI^{z+}} &= \frac{[L_nI^{z+}]}{[I^{z+}][L]^n} \end{aligned} \quad . \qquad 13.$$

Multiplying the exchange constant for the single ions $K_{exch}^{H^+,I^{z+}}$ with the complex formation and acidity constant yields the overall exchange constant $K_{exch}^{IndH^+,L_nI^{z+}}$:

$$\begin{aligned} K_{form/diss}K_{exch}^{H^+,I^{z+}} &= (K_a)^z\beta_{L_nI}K_{exch}^{H^+,I^{z+}} \\ &= \left(\frac{[Ind^0][H^+]}{[IndH^+]}\right)^z \frac{[L_nI^{z+}]}{[I^{z+}][L]^n}\frac{(a_H)^z[I^{z+}]}{[H^+]^z a_I} = \left(\frac{[Ind^0]a_H}{[IndH^+]}\right)^z \frac{[L_nI^{z+}]}{[L]^n a_I} = K_{exch}^{IndH^+,L_nI^{z+}}. \end{aligned} \qquad 14.$$

Therefore, the overall exchange constant may be replaced by the product of the exchange constant of the naked ions, the complex formation constant, and the dissociation constant to the power of

the primary ion's charge. The response function in Equation 10 can thus be equally formulated as

$$a_I = \frac{1}{z(K_a)^z \beta_{L_nI^{z+}} K_{exch}^{H^+,I^{z+}}} \left(\frac{a_H \alpha}{1-\alpha}\right)^z \frac{R_T - (1-\alpha)Ind_T}{\{L_T - z^{-1}n[R_T - (1-\alpha)Ind_T]\}^n}. \quad 15.$$

Using software such as Mathematica, Matlab, or Excel, investigators can use this equation to predict the sensor response under different parameters.

Although this approach is valuable for simulating the response of a certain IBOS to changing ionophores or lipophilic indicators, a problem arises if $K_{exch}^{H^+,I^{z+}}$ is unknown. For the primary target ion, the value may be calculated using K_a and $\beta_{L_nI^{z+}}$ values known from the literature and the obtained overall exchange constant $K_{exch}^{IndH^+,L_nI^{z+}}$ from curve fitting with Equation 10. However, separately measuring $K_{exch}^{H^+,I^{z+}}$ would be more convenient because it is a constant for a certain combination of the target ion and proton in a defined sensor matrix. To obtain these values, electrochemical methods are preferred because they enable the exchange constants to be determined without additional ionophores or optical reporter dyes (84). A membrane consisting of an ionic additive, plasticizer, and supporting polymer will readily supply the value of $K_{exch}^{H^+,I^{z+}}$ for the various combinations of ions by measuring the standard potential (E^0) in a separate solution experiment (see Reference 74 for more details). The extrapolated potentiometric signal at 1 M after fitting of the potential response in the Nernstian response region with the theoretical equation for the various solutions allows for the calculation of K_{IJ}^{pot}, which corresponds to the unbiased exchange constant at the interface. Although examples of these selectivities with different combinations of plasticizers and ions can be found in the literature, no comprehensive list combines all these data sets into a single source.

3.3. Response in the Presence of Interfering Ions

So far, the response function has considered only the response without interfering ions. Although it is still very useful for understanding the different parameters contributing to the IBOS response, real samples contain secondary ions that compete with the primary ions for binding sites in the optode membrane. The above model can be extended to cases where secondary ions J of charge z_J compete with primary ions I of charge z_I. The resulting complexes with the ionophore L have the stoichiometries n_I and n_J, respectively. Separate exchange equilibria for each ion can be described as

$$z_I IndH^+(org) + n_I L(org) + I^{z_I+}(aq) \rightleftharpoons z_I Ind^0(org) + L_{n_I} I^{z_I+}(org) + z_I H^+(aq)$$

$$z_J IndH^+(org) + n_J L(org) + J^{z_J+}(aq) \rightleftharpoons z_J Ind^0(org) + L_{n_J} J^{z_J+}(org) + z_J H^+(aq).$$

This results in two separate overall ion exchange constants:

$$K_{exch}^{IndH^+,L_{n_I}I^{z_I+}} = \frac{[Ind^0]^{z_I}(a_H)^{z_I}[L_{n_I}I^{z_I+}]}{[IndH]^{z_I}[L]^{n_I}a_I(IJ)}; \quad 16.$$

$$K_{exch}^{IndH^+,L_{n_J}J^{z_J+}} = \frac{[Ind^0]^{z_J}(a_H)^{z_J}[L_{n_J}J^{z_J+}]}{[IndH]^{z_J}[L]^{n_J}a_J(IJ)}. \quad 17.$$

The letters "IJ" in brackets after the activity indicate the activities in a solution that contain both primary and interfering ions. Although the mass balance for the indicator (Equation 6) and the definition of the protonation degree (Equation 5) still hold, the mass and charge balance have to be extended to develop the response function for the primary ion directly:

$$L_T = [L] + n_I[L_{n_I}I^{z_I+}] + n_J[L_{n_J}J^{z_J+}]; \quad 18.$$

$$R_T = z_I[L_{n_I}I^{z_I+}] + z_J[L_{n_J}J^{z_J+}] + [IndH^+]. \quad 19.$$

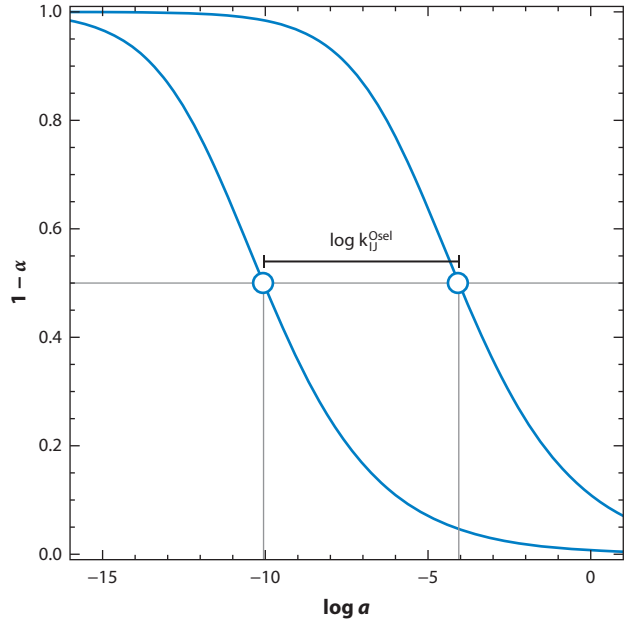

Figure 5

Graphical representation of the selectivity of ionophore-based optical sensors.

This equation system is significantly more complex than the single ion response function developed above. Obtaining the analytical solution requires known complex stoichiometries and is somewhat tedious. For the development of an exact solution, the interested reader is referred to the **Supplemental Text** (for all **Supplemental Material**, follow the link from the Annual Reviews home page at **http://www.annualreviews.org**).

Supplemental Material

The need for simplification has resulted in the development of a model that not only describes the selectivity of IBOS in a more intuitive manner but also can be generalized for all stoichiometries and ion charges. Considering a practical characterization concerning selectivity of the primary ion I over an interfering ion J, one approach is to measure the response in terms of $1 - \alpha$ versus log a in a separate solutions method. The selectivity $\log k_{IJ}^{Osel}$ is a product of the distance of the two curves at a given protonation degree, typically $1 - \alpha = 0.5$ (see **Figure 5**) (85, 86).

This can be expressed mathematically as

$$k_{IJ}^{Osel} = \frac{a_I(I)}{a_J(J)} \quad \text{or} \quad \log k_{IJ}^{Osel} = \log a_I(I) - \log a_J(J). \qquad 23.$$

By contrast, the activity of the primary ion in the mixed solution $a_I(IJ)$ can be considered as the activity without interfering ions $a_I(I)$ reduced by the activity of the interfering ion weighted by the selectivity factor k_{IJ}^{Osel}:

$$a_I(IJ) = a_I(I) - k_{IJ}^{Osel} a_J(IJ). \qquad 24.$$

Hence, the response function in mixed solutions can be expressed by inserting Equations 15 (expressed for I and J) and 23 into Equation 24:

$$a_I(IJ) = \frac{1}{z_I (K_a)^{z_I} \beta_{L_n I^{z+}} K_{exch}^{H^+, I^{zI+}}} \left(\frac{a_H \alpha}{1 - \alpha} \right)^{z_I} \frac{R_T - (1 - \alpha) Ind_T}{\{L_T - z_I^{-1} n_I [R_T - (1 - \alpha) Ind_T]\}^{n_I}} - k_{IJ}^{Osel} a_J(IJ), \qquad 25.$$

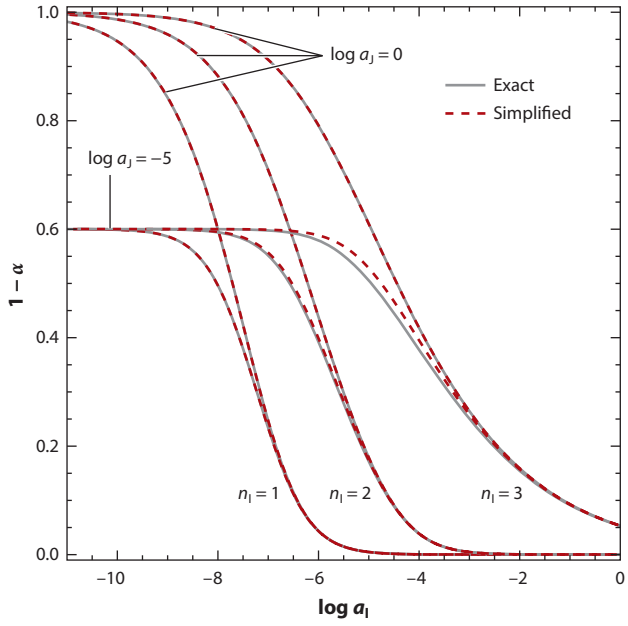

Figure 6

Supplemental Material

Comparison of exact (**Supplemental Equation 9**) and simplified (Equations 25 and 26) solutions of the response function for different cases. The complex stoichiometry for the interfering ion (n_J) as well as the charges of both ions z_I and z_J were set to 1. Membrane composition: $Ind_T = R_T = \frac{1}{3}L_T$. Other parameters (pH, K_a, β, K_{exch}) have been adjusted to achieve $1 - \alpha = 0.6$ for $\log a_J = -5$.

with

$$k_{IJ}^{Osel} = \frac{a_I(I)}{a_J(J)} = \frac{z_J \beta_{L_{n_J} J^{z+}} K_{exch}^{H^+, J^{zJ+}}}{z_I \beta_{L_{n_I} I^{z+}} K_{exch}^{H^+, I^{zI+}}} \left(\frac{1}{K_a} \frac{a_H \alpha}{1 - \alpha} \right)^{z_I - z_J} \frac{\left\{ L_T - z_J^{-1} n_J [R_T - (1 - \alpha) Ind_T] \right\}^{n_J}}{\left\{ L_T - z_I^{-1} n_I [R_T - (1 - \alpha) Ind_T] \right\}^{n_I}}. \quad 26.$$

Graphical comparison of the results for different values of n_I show that a slight difference between the output of the exact (**Supplemental Equation 9**) and the simplified (Equations 25 and 26) solutions is observed only for larger values of the complex stoichiometry and in the presence of significant interfering ion activity (**Figure 6**). The possibility of generalizing the simplified model outweighs the slight deviation. Thus, Equations 25 and 26 are recommended for fitting the experimental data.

3.4. Detection Limit of IBOS

The lower detection limit of IBOS cannot be described in a universal way because it depends on different factors. The detection limit can, for instance, be dictated by the following:

- Interference from other ions (interfering ion dominates over primary ion)
- The noise level of the instrument
- Loss of sensitivity due to the sigmoidal shape of a response curve
- Analyte depletion (e.g., a measurement changes the analyte concentration in a sample, response time is too long).

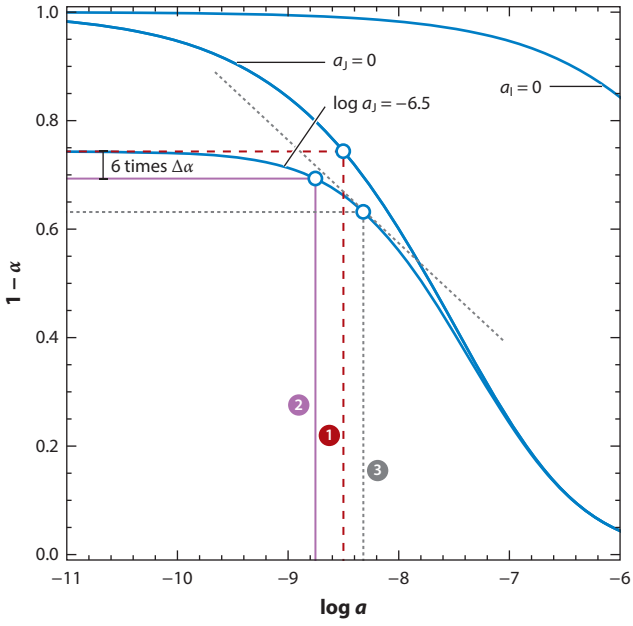

Figure 7

Detection limits based on ① interference from the background, ② instrumental noise level, or ③ loss of sensitivity (threshold slope).

In case 1 in **Figure 7**, the detection limit $a_I(\mathrm{DL})$ can be predicted by the activity of the interfering ion a_J and the selectivity coefficient k_{IJ}^{Osel} according to

$$a_I(\mathrm{DL}) = k_{IJ}^{Osel} a_J. \qquad 27.$$

This is equivalent to the ion activity of a response curve without an interfering ion at a protonation degree equal to the maximal protonation degree when no primary ion but only an interfering ion is present (see **Figure 7**). A more practical definition of the detection limit (case 2 in **Figure 7**) can be given by transforming the noise level of the instrumentation into a $\Delta\alpha$ value. Then, 6 times $\Delta\alpha$ is usually subtracted from the maximum $1-\alpha$ in the mixed solution (background ions only), and the intersection of a horizontal extrapolation with the response function determines the lower limit of detection. Sometimes, the detection limit is also defined by the requirement of a minimum sensitivity (slope of the response function) (case 3 in **Figure 7**).

Finally, an effective limit of detection is also observed as a result of the required extraction of analyte to the bulk of the IBOS. The minimally required change of protonation degree requires a certain amount of analyte, and at low concentration or low sample volume, this may result in a limitation from the sample side. As such, either a significant change in the sample composition owing to the measurement or an unacceptable response time defines the lower limit of detection.

Because most detection limits are directly or indirectly influenced by the sigmoidal shape of the response curve, researchers recently tried to increase the dynamic measurement range using a mathematical linearization method, i.e., logit linearization (see Reference 29). By plotting the logarithm of $(1-\alpha)/\alpha$ versus $\log a_I$, the authors achieved an increase of the measuring range from the typical 3 to 8 orders of magnitude. Although a mathematical linearization cannot overcome the limitation given by the instrumental noise or the limitation due to background ions or sample depletion and should not be combined with traditional least-squares weighting of the data, this method represents a convenient simplification of the readout of IBOS.

The total measuring range can be described as the region between the upper and lower detection limits. The upper detection limit can be understood as an increase of ion-exchanger site concentration owing to the coextraction of the electrolyte, but this has not been studied in great detail (30). The sigmoidal response curve still implies a loss of sensitivity close to the upper detection limit, which can be quantified by analogy to cases 2 and 3 in **Figure 7**. However, highly lipophilic ions in the sample can cause nonspecific coextraction, which shifts the practical measuring range. For a cation-specific IBOS based on ion exchange, electroneutrality in the sensing phase would be maintained by coextracting the lipophilic anions together with the target cation in parallel with the desired exchange of protons bound to the indicator dye.

Measuring ranges defined by a limiting slope of the response curve can be calculated from the response function. The range in terms of analyte concentration depends drastically on the sensor composition, complex stoichiometry, and charge of the involved ions. However, the protonation degree in all cases is between 0.1 and 0.9. In general, the slope of the response curve decreases with increasing charge z and complex stoichiometry n of the ions (25).

3.5. Response Time of IBOS

For equilibrium-based IBOS, the necessity of extracting the analyte into the bulk of the membrane results in significantly longer response times than achieved via comparable surface- or interface-based techniques, such as ionophore-based ion-selective electrodes. The response time of most commonly used membranes, i.e., plasticized PVC [poly(vinyl chloride)] with a thickness of several micrometers, is usually dominated by the diffusion time in the bulk of the membrane. Simplifying this case by assuming an average, concentration-independent diffusion coefficient D_m in the membrane results in a simple relationship between the square of the membrane thickness and the response time (25):

$$t_{95} = 1.13 \frac{d^2}{D_m}. \qquad 28.$$

Using typical diffusion coefficients for ionic species in such membranes of $D_m \approx 10^{-8}$ cm^2 s^{-1} results in a response time of approximately 1 s for a film of 1-μm thickness. Note that spherical IBOS particles instead of planar film optodes may decrease the response time substantially because of spherical diffusion.

However, the limitation of the diffusion in the membrane phase is given only at relatively high analyte concentrations. Lerchi et al. (53, 87) observed earlier that the response time of extremely sensitive IBOS for heavy metals is mainly dependent on mass transport in the solution. As a result of extremely enhanced mass transport through the large surface/volume ratio of the nanoparticles, the application of small IBOS nanoparticles in well-mixed suspension should overcome this problem. Finally, reducing the amount of active compounds in IBOS also results in a decreased response time. However, the lower sensitivity of absorbance-based measurements, in particular, results in an instrumentation-based limit. Employing fluorescent dyes provides intrinsically higher sensitivity.

Lessons to learn from theoretical response curves include the following:

- The response function can be utilized to fine-tune and predict the influence of IBOS composition on the sensor characteristics in equilibrium mode.
- Independent ionophore and lipophilic indicator optimization allows for maximized flexibility in the design of optical ion sensors.
- pH dependency of the response can be exploited to tune the responsive range of IBOS.
- IBOS usually respond slower than do surface optodes or potentiometric sensors, but new particle-based techniques will likely overcome this limitation in the near future.

4. SENSOR CONFIGURATIONS AND INSTRUMENTAL ASPECTS

4.1. Absorbance Readout Mode

Absorbance is by far the most applied readout concept in IBOS research today. Especially in the early years, most groups relied on absorbance because of the robust, cost-effective, and simple instrumentation. The direct correlation between the absorbance and concentration of the absorbing species through Lambert-Beer's law also provides a straightforward correlation of the protonation degree and the physical signal of an IBOS. Moreover, the absorption of light by a lipophilic pH indicator can be exploited in many different ways. Although measuring IBOS using thin films coated onto glass or quartz slides in transmission mode is still used for fundamental studies, the drawbacks of relatively bulky equipment and limited portability stimulated researchers to explore different concepts. Another disadvantage of measuring in transmission mode is the inverse correlation of signal and response time: Thin films result in a shorter response time but lower signal. In fact, the response time increases with the square of film thickness, whereas the signal is directly proportional to it. The limit in thickness is given by the minimum amount of dye molecules in the optical path required for obtaining a reliable signal. The question is therefore: How can one improve the optical signal without increasing the film thickness? In theory, there are at least three different ways: (*a*) maximizing the concentration of dye in the sensor, (*b*) applying indicators with a high molecular absorption coefficient ε_λ, and (*c*) maximizing the optical path length without increasing the membrane thickness. The first approach is simple but limited by the solubility of the dye in the matrix material. Similarly, applying high-ε_λ indicators is obvious, but the availability of lipophilic pH indicator dyes sets a limit here as well. An ideal indicator for IBOS is highly soluble in the matrix material, has a high ε_λ, and is also poorly soluble in the sample solution. The latter aspect is important to avoid leaching of the dye from the sensor. Finally, increasing path length without increasing film thickness can be achieved by changing the geometry of the readout. Instead of sending the light perpendicular through the film, it is beneficial to guide the light through a thin film or exploit the evanescent wave of light in a total internal reflection mode. Suzuki and coworkers (35) evaluated these two approaches for IBOS and other groups later employed them to produce IBOS with improved sensitivity (64, 88–91). Especially the active waveguide approach in which the light passes through the IBOS film shows a very attractive sensitivity improvement owing to the increased path length of the light. However, the response time is still governed by the diffusion perpendicular to the membrane. A similar approach can be taken by using a porous material with a high specific area to obtain a faster equilibration of the sensing phase with the sample. This was, for instance, realized by coating an IBOS cocktail onto porous microparticles (31, 36).

When we observe the response of an IBOS to a changing analyte concentration, we see a combination of transmission and reflection signal. Hence, it should also be possible to quantitate the sensor response by mimicking the human eye. A number of reports describing such approaches have been published, and this concept has recently gained interest in the scientific community. Reflection as the readout mode has several advantages over transmission. Primarily, the optics of the light source and detection can be located on the same side of the sample. Thus, this allows for the application of bifurcated fiber bundles to the readout of immobilized particles coated with an IBOS film (31, 36, 85). Furthermore, opaque or turbid sensors are no longer problematic because the background due to light scattering by the sample in transmission mode is less disturbing. This is also beneficial for disposable test-strip sensors, whose employment for optical detection of various compounds using reflectometric photometers such as the Seralyzer occurred long before the real advent of IBOS (92, 93). Finally, low-cost pieces of equipment, such as digital cameras and

scanners, have become attractive tools to replace costly spectrophotometric equipment. Especially in recent years, the adaptation of the well-understood IBOS theory to low-cost, easy to use optical ion sensors has become a prominent topic in research. Johnson et al. (12), for instance, presented a highly developed yet simple centrifugal microfluidic platform with integrated IBOS. The device was designed to be operated using both mechanics and optics of conventional DVD players.

Note that once the characteristics of an optical sensor in contact with a sample are well understood, it will also be possible to develop low-cost equipment for transmission-based sensors. A full spectral characterization is no longer required. In fact, even referenced sample readout is possible with measurement at only two wavelengths. Researchers (94) have developed portable photometers in which LEDs (light-emitting diodes) and photodiodes are employed as light sources and detectors. Such devices have been applied to measure both cations (95) and anions (96) in real samples. In applications where qualitative or semiquantitative information about the analyte concentration is sufficient, so-called naked-eye sensors represent an attractive alternative to the instrumental approach for signal readout. Here, IBOS are optimized to show maximum color change in the appropriate concentration range of the analyte. Such ionophore-based optodes can provide information on the transition metal content in aqueous samples (97). Nevertheless, the new trend toward the ubiquity of mobile devices with powerful digital cameras has stimulated researchers to exploit this technology for optical chemical sensors. The Capitán-Vallvey group (40, 98, 99), in particular, has made tremendous efforts to establish the necessary basis to allow a reliable and flexible yet simple readout of IBOS using such devices.

4.2. Fluorescence Readout Mode

The availability of fluorescent lipophilic pH indicators has had a tremendous effect on the applicability of IBOS to various applications. Owing to their intrinsically higher sensitivity, less-active components are necessary for obtaining reliable signals. Hence, thinner-film optodes can be employed to reduce the response time and, in theory, the limit of detection. Moreover, fluorescence measurements allow, similar to reflectance or colorimetric readout, the location of both the excitation source and detector on the same side of the sample. Although few reports discuss absorbance measurements on particle beds (85) or single microparticles (100), multiplexed particle arrays (101), flow cytometric applications (13, 14), as well as nanoparticles for imaging applications (4, 102, 103) depend solely on fluorescence as a detection technique. The first miniaturized IBOS based on optical fibers with coated tips were also based on fluorescence (5, 104), although here a combination of absorbance and fluorescence based on an inner-filter effect was applied. This is a convenient way to transform an analyte-dependent absorbance signal of a nonfluorescent pH indicator into a fluorescence signal. Provided that there is a good spectral overlap between the absorbance band of the indicator and the emission band of a nonresponsive, luminescent reporter dye, the emission signal can be reabsorbed by the indicator dye. Hence, a change in absorbance directly translates into a change in the fluorescence signal. IBOS in various formats have been reported on the basis of this system, most often employing the fluorescent reporter 1,1′-dioctadecyl-3,3,3′,3′-tetramethylindocarbocyanine perchlorate (DiIC18) in combination with Nile blue derivatives such as ETH 5418 or ETH 5294 (5, 15, 105). In fact, many combinations of reporter and indicator dye are suitable, provided they show appropriate spectral overlap and sufficient solubility in the matrix material. Recently, Xie et al. (16, 106) introduced an exciting variant of this approach. They employed dual-emission upconverting nanorods as the infrared-excitable reporter. Interestingly, the two emission bands show perfect overlap with both bands (acidic and basic) of lipophilic Nile blue derivatives such as ETH 5418 and ETH 5294. This means that the emission of the nanorods at two distinct wavelengths can be absorbed by the different absorbance bands of the indicator dye.

Therefore, a direct transduction of the full ratiometric behavior of the indicator to an otherwise nonresponsive fluorescent reporter is possible.

4.3. Other Readout Modes

Besides the two main readout modes for IBOS, i.e., fluorescence and absorbance, other techniques such as refractive index or surface plasmon resonance (SPR) have been successfully applied. Freiner et al. (107), for instance, proposed a waveguide setup where the refractive index of an IBOS film changes upon analyte binding. This variation was then translated into an apparent change of the underlying waveguide, thereby altering the output signal. Kurihara et al. (108) spin-coated conventional SPR chips with a cocktail to develop SPR-based IBOS. Later, the same group (109) discovered that the conical shape of gold-coated, chemically edged optical fibers also allows for the generation of SPR.

4.4. Referencing Concepts

Compared with electrochemical sensors, optochemical sensors have certain advantages in terms of signal stability. However, the utilization of light as a transducing mechanism also introduces unique problems. Independent of the type of signal collected (absorbance or fluorescence), the signal intensity depends on various factors such as the intensity of the light source, the concentration of the dye, detector sensitivity, loss of intensity in light-guiding material, sample turbidity, and background signal from the sample, among many others. As such, designing and making an IBOS that responds to the analyte concentration is fairly straightforward, but designing a robust yet simple IBOS is much more challenging. Fortunately, there are several referencing techniques where the analyte-dependent signal is related to a second signal that may or may not be analyte dependent. In these cases, many of the above-mentioned optical interferences can be corrected, given that these interferences affect both signals in the same way.

4.4.1. Ratiometric referencing. The combination of a luminescent lipophilic pH indicator and a luminescent reference dye, for instance, would yield a system that is stable against all changes concerning the intensity of the excitation light (see **Figure 8**). Here, the intensity ratio at the two wavelengths can be used as a signal and replaces the intensity at the analyte-dependent wavelength. A change in excitation intensity, for instance, would affect both peaks in the same way; therefore, no signal change would be detected. However, a change in analyte concentration should affect only the peak of the indicator dye. In this case, the protonation degree can be calculated in complete analogy to a single wavelength readout because all signal S_{max}, S_{min}, and S are divided by the same analyte-independent reference signal S_{ref}. Hence, for a system with increasing signal intensity at increasing protonation degree $1 - \alpha$, the following expressions are valid:

$$R_{max} = S_{max}/S_{ref}, \quad R_{min} = S_{min}/S_{ref} \quad \text{and} \quad R = S/S_{ref}; \tag{29.}$$

$$1 - \alpha = \frac{S - S_{min}}{S_{max} - S_{min}} = \frac{S/S_{ref} - S_{min}/S_{ref}}{S_{max}/S_{ref} - S_{min}/S_{ref}} = \frac{R - R_{min}}{R_{max} - R_{min}}. \tag{30.}$$

A different ratiometric referencing scheme can be used for dual-emission or dual-absorbance dyes (110). Here, both spectral bands depend on the protonation degree of the indicator, but in opposite ways. A prominent example of such a dye is the Nile blue derivative ETH 5418 for which the correlation of the protonation degree and the ratiometric value has to be considered. ETH 5418 exhibits an absorbance peak S_1 at $\lambda_1 = 540$ nm that decreases and another peak at $\lambda_2 = 590$ nm (S_2) that increases with increasing protonation. The protonation degree can now be expressed in

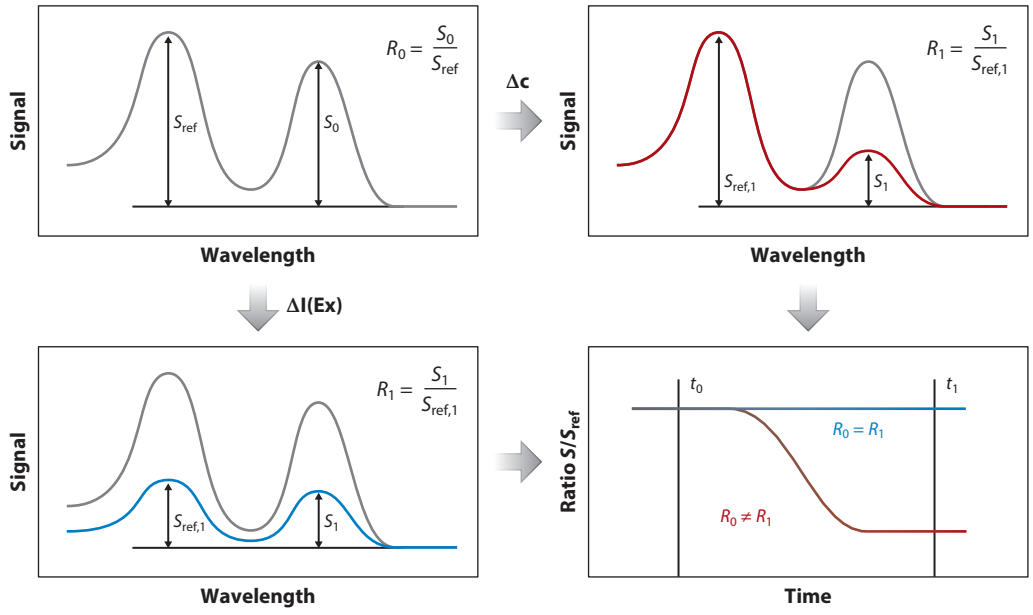

Figure 8

Dual-wavelength referencing. Protonation of the indicator influences only the signal S at the longer wavelength, whereas S_{ref} is independent of the analyte concentration a_1. A change in excitation intensity triggers no change in the intensity ratio.

two ways:

$$1 - \alpha = \frac{S_{1,max} - S_1}{S_{1,max} - S_{1,min}}; \tag{31.}$$

$$1 - \alpha = \frac{S_2 - S_{2,min}}{S_{2,max} - S_{2,min}}. \tag{32.}$$

If the ratio is formed by always dividing the signal at λ_2 by the signal at λ_1,

$$R = S_2/S_1 \tag{33.}$$

and

$$R_{max} = S_{2,max}/S_{1,min} \quad R_{min} = S_{2,min}/S_{1,max}. \tag{34.}$$

Solving Equations 31 and 32 for S_1 and S_2, respectively, inserting the results in Equation 33, and solving for $1 - \alpha$ gives

$$1 - \alpha = \frac{S_{2,min} - RS_{1,max}}{R(S_{1,min} - S_{1,max}) - S_{2,max} + S_{2,min}}. \tag{35.}$$

After replacing $S_{2,max}$ and $S_{2,min}$ in Equation 35, using Equation 34, and rearranging the resulting equation, $1 - \alpha$ can be expressed as

$$1 - \alpha = \frac{(R - R_{min})SF}{R_{max} + R(SF - 1) - R_{min}SF} = 1 - \left(1 + SF\frac{R - R_{min}}{R_{max} - R}\right)^{-1}, \tag{36.}$$

where SF is the scaling factor

$$SF = S_{1,max}/S_{1,min}. \tag{37.}$$

It is important to note that the scaling factor is always the ratio of signal at the wavelength used as the denominator in Equation 33, i.e., the referencing signal. Moreover, Equation 36 also holds

when the intensity at the reference wavelength is independent of the analyte concentration (see **Figure 8**), because the scaling factor becomes 1 and Equation 36 becomes Equation 30. The above-mentioned equations hold for both absorbance and luminescence readout schemes.

4.4.2. Decay time and colorimetric approaches. Although most referenced IBOS are obtained using the above-mentioned ratiometric approach, other approaches may be used to obtain robust signals from optical sensors. Environmental background light, for instance, can be efficiently suppressed by using a modulated excitation light. Consequently, subtracting a nonmodulated background from the modulated signal of the IBOS becomes a straightforward task, and the signal-to-noise ratio is greatly increased even at a low signal intensity. Although this is a well-known and established technique for background subtraction in optical devices, readout of IBOS with modulated signals has been carried out only using commercial modulated spectrophotometers. A more sophisticated technique for referencing is the application of fluorescent indicators with a pH-dependent decay time (or lifetime). The decay time of a fluorophore is an intrinsically referenced signal because it does not depend on intensity-influencing factors such as the excitation light or the concentration of the indicator dye, so long as the dye concentration does not change the response function developed in Section 3. If a fluorescent lipophilic pH indicator with such properties is employed, vastly enhanced performance of the IBOS is expected. Time-resolved fluorescence pH measurements have been demonstrated using resorufin with a pulsar technique (111) and using an immobilized carboxy seminaphthofluorescein-1 in the frequency domain (112). A detailed discussion of decay-time techniques is omitted here because, to the best of our knowledge, these techniques have not yet been employed for IBOS. The main reason for this may be the relatively expensive equipment required for measuring decay times in the nanosecond range. However, measurements in the frequency domain may be an attractive option for IBOS, especially for biological imaging where background fluorescence often hampers reliable readout of optical sensors.

An interesting development that, in some way, is a combination of both ratiometric and lifetime referencing techniques is the so-called dual-lifetime referencing approach (113). Here, a fluorescent pH indicator can be combined with a phosphorescent reference dye, preferably one with otherwise similar spectral characteristics. When this combination of dyes is excited with a sinoidally modulated light source, the resulting emission light is modulated by the same frequency. However, the output will have a certain phase shift compared with that of the excitation source.

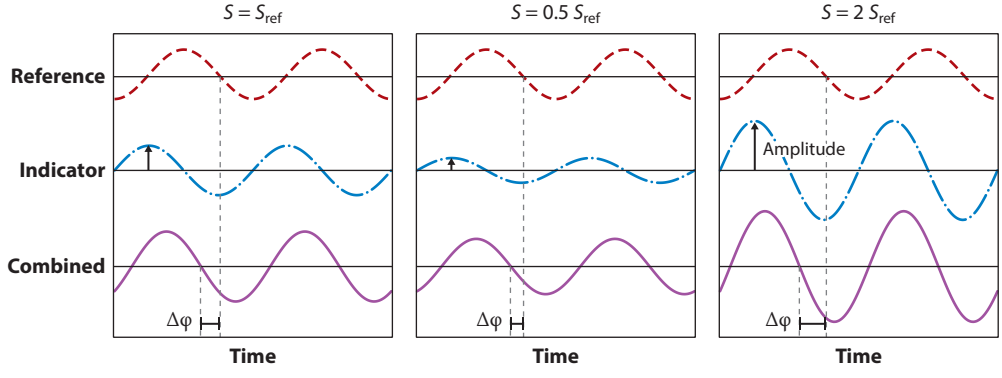

Figure 9

Correlation of the phase shift Δφ with the amplitude of the light emitted from the indicator dye in a dual-lifetime referencing scheme.

Because the resulting phase shift is proportional to the intensity ratio of both dyes, a frequency that is adapted to show the maximal phase shift of the reference dye may be chosen and the phase shift may be correlated to the protonation degree of the pH indicator (see **Figure 9**). The advantage of this approach is the possibility of measuring lifetimes in the micro- to millisecond range, which, compared with fluorescence decay-time measurements, greatly reduces instrumental complexity. Interestingly, there are no reports so far on the successful application of this approach using IBOS, although it was introduced using ion sensors based on a hydrogel immobilized chloride indicator (113). We expect that decay-time-based referencing schemes will find their way into the applied research of IBOS in the near future.

Reflectometric measurements can also be referenced by comparing the diffuse reflectance of an analyte-sensitive IBOS spot with a simultaneously evaluated spot that is free of colored species,

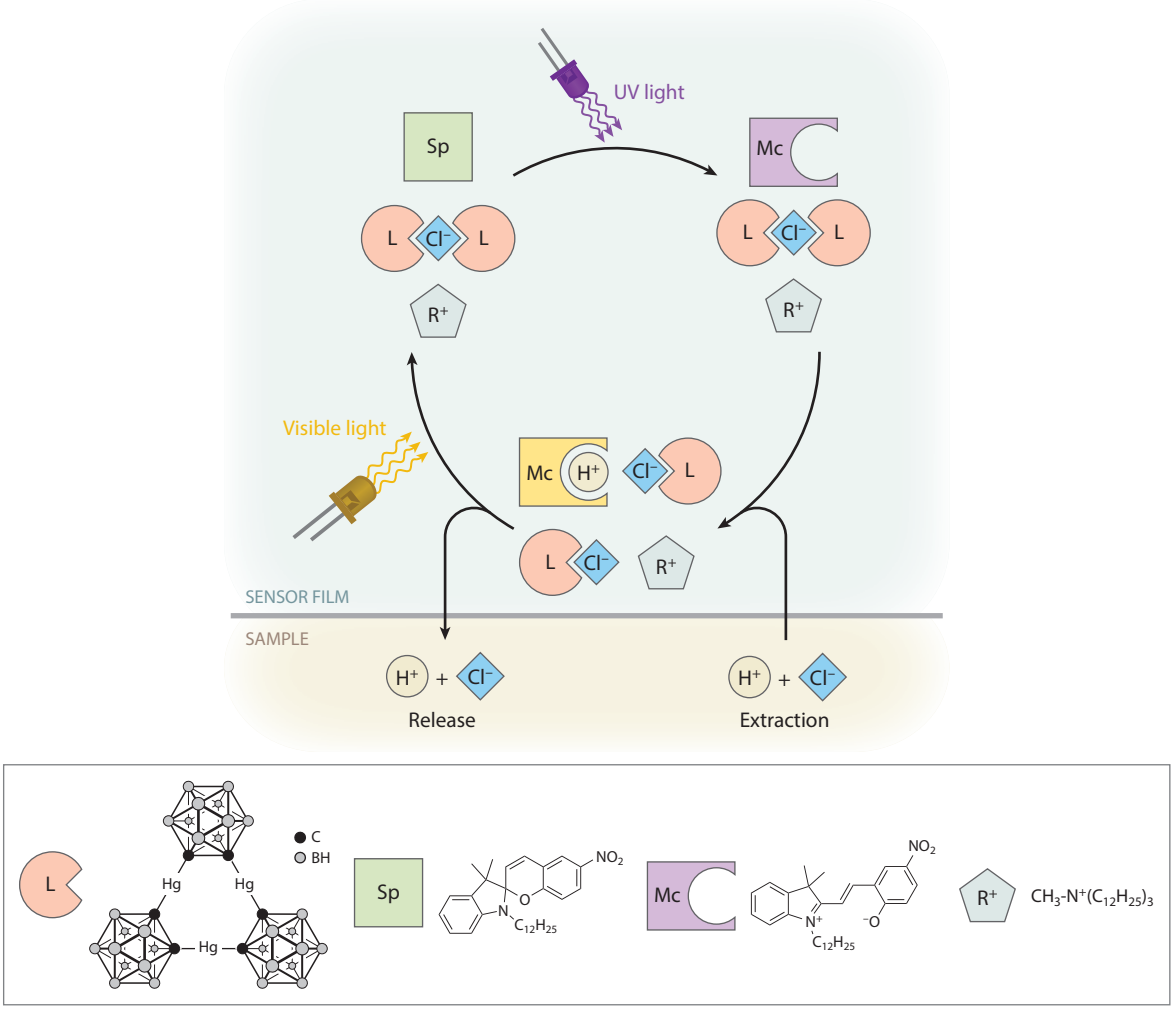

Figure 10

Schematic of a light-responsive ionophore-based optical sensor selective for chloride.

i.e., is white. Here, the relative reflectance signal $S_{rel} = S_{sens}/S_{ref}$ is not directly proportional to the analyte concentration, but it can be transformed into the Kubelka-Munk function $f(S_{rel})$, which is proportional to the concentration of the colored species (e.g., c_{IndH^+}) according to

$$f(S_{rel}) = \frac{(1 - S_{rel})^2}{2S_{rel}} = kc_{IndH^+}. \qquad 38.$$

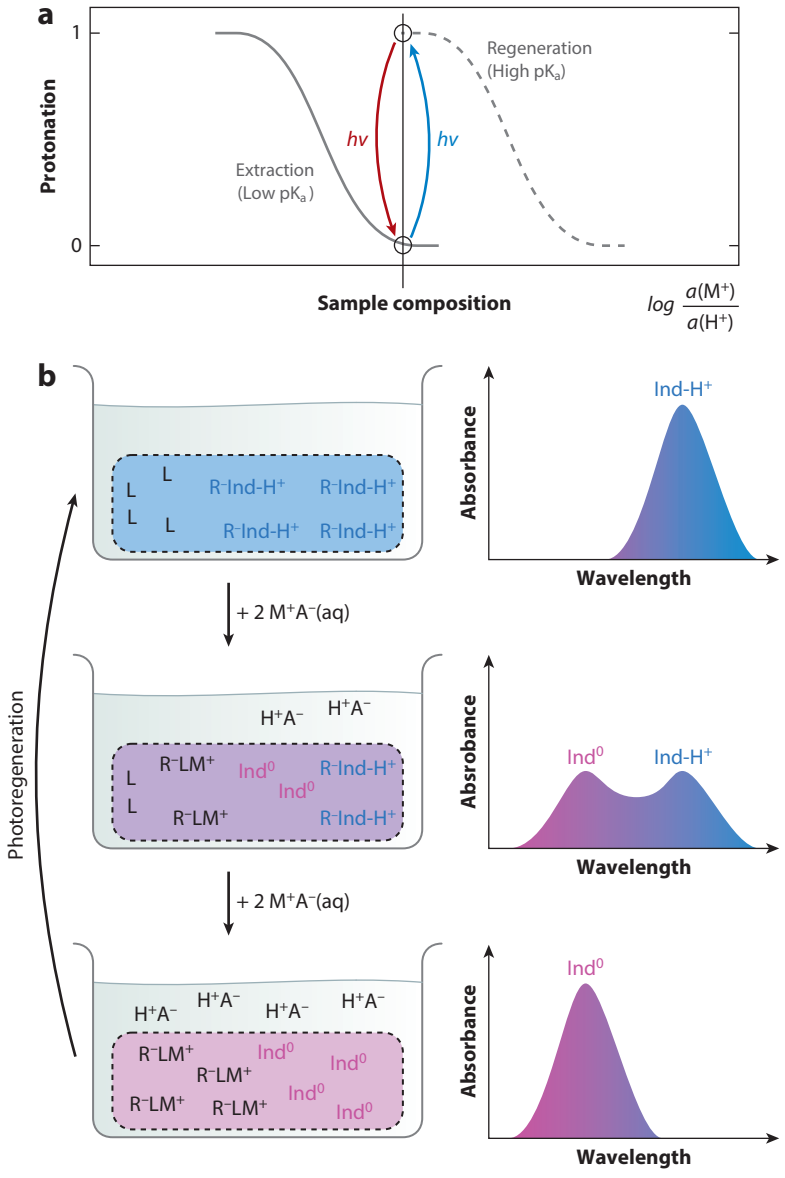

Figure 11

Photoregeneration of an exhaustive-exchange ionophore-based optical sensor, which will extract all available analyte cations (M^+) from a sample. Illumination then regenerates the original, receptive state of the sensor. Abbreviations: A^-, anion; Ind, lipophilic pH-indicator; L, ionophore; R^-, anionic site.

Tohda et al. (114, 115), among others, have developed an exciting application for this concept. They established a colorimetric readout of IBOS for multianalyte sensing in the interstitial space of human skin.

A relatively new and promising technique, especially for low-cost equipment, is the evaluation of the hue value *H* of the HSV (hue, saturation, value) color space as an analytical signal in bitonal optical sensors. The *H* value represents the color of a material and should be independent of factors that determine the signal intensity, such as film thickness and illumination light intensity, making it an attractive physical property to correlate with analyte concentration. Although conventional imaging devices usually generate images in the RGB (red, green, blue) color space, it is fairly straightforward to calculate *H* from the different intensities in the RGB space. Cantrell et al. (116) demonstrated that the *H* value is surprisingly more robust than simple two-channel ratiometric measurements in bitonal IBOS.

5. CURRENT DEVELOPMENTS IN IBOS: PHOTODYNAMIC SENSORS

Recently, researchers introduced a new concept concerning dynamic optical ion sensors based on the replacement of IBOS components with light-responsive analogs. The pK_a value of the pH indicator or the complex formation constant of the ionophore in an IBOS, for instance, has a direct effect on the response function (see Section 3.2). Therefore, a dynamically changing sensor response may be anticipated via the introduction of a pH indicator, which changes its pK_a value in response to an external stimulus. One especially promising example is spiropyran: Upon irradiation with UV light, spiropyran increases its apparent pK_a value in a plasticized PVC membrane by more than six orders of magnitude (84). In addition to its dynamically changeable affinity for protons, this compound exhibits a fluorescence spectrum that depends on the protonation degree, making it a suitable pH indicator for dynamic IBOS. Exploiting this property, we designed a switchable IBOS for chloride (117), sodium, and calcium (118). A schematic representing this sensor is shown in **Figure 10**.

So far, this concept has been used to switch an IBOS from a nonequilibrium to an equilibrium mode, thereby changing the dynamic IBOS from a state where ion exchange or coextraction was blocked ("off") to a responsive state ("on"). Other cases are imaginable: Switching could trigger a more severe jump in the response. Changing the affinity for one of the ions involved so that the final state is on the other extreme of the response curve would yield an exhaustive exchange system, as explained in Section 2.1, although a dynamic regeneration step is now possible (see **Figure 11**). It is important to note that a huge dynamic shift in the response curve implies a huge shift in the affinity of one of the active components for its respective target ions. As such, this concept relies on the availability of molecules that allow for a phototriggered change in affinity.

SUMMARY POINTS

1. The availability of response functions for different types of IBOS greatly facilitates the identification of crucial parameters in sensor design.
2. A robust and easy to use IBOS requires an intelligent referencing scheme. Although ratiometric referencing is usually simple to achieve, intrinsically referenced signals, such as luminescence decay time, should be applied more often for IBOS in the near future.

3. Despite the long history of IBOS, new and exciting concepts and extensions to conventional techniques are regularly introduced into the field. For example, IBOS with photoactive compounds allow IBOS applications otherwise impossible with static IBOS components.

DISCLOSURE STATEMENT

The authors are not aware of any affiliations, memberships, funding, or financial holdings that might be perceived as affecting the objectivity of this review.

ACKNOWLEDGMENTS

The authors thank the University of Geneva and the Swiss National Science Foundation for financial support. G.M. gratefully acknowledges the support of the Austrian Science Fund (FWF): J3343.

LITERATURE CITED

1. Meier RJ, Schreml S, Wang X, Landthaler M, Babilas P, Wolfbeis OS. 2011. Simultaneous photographing of oxygen and pH in vivo using sensor films. *Angew. Chem.* 123(46):11085–88
2. Ungerböck B, Charwat V, Ertl P, Mayr T. 2013. Microfluidic oxygen imaging using integrated optical sensor layers and a color camera. *Lab Chip* 13(8):1593
3. Glud RN, Tengberg A, Kühl M, Hall POJ, Klimant I, Holst G. 2001. An in situ instrument for planar O_2 optode measurements at benthic interfaces. *Limnol. Oceanogr.* 46(8):2073–80
4. Harjes DI, Dubach JM, Rosenzweig A, Das S, Clark HA. 2010. Ion-selective optodes measure extracellular potassium flux in excitable cells. *Macromol. Rapid Commun.* 31:217–21
5. Shortreed M, Bakker E, Kopelman R. 1996. Miniature sodium-selective ion-exchange optode with fluorescent pH chromoionophores and tunable dynamic range. *Anal. Chem.* 68:2656–62
6. Citterio D, Takeda J, Kosugi M, Hisamoto H, Sasaki S, et al. 2007. pH-independent fluorescent chemosensor for highly selective lithium ion sensing. *Anal. Chem.* 79:1237–42
7. Watts AS, Urbas AA, Moschou E, Gavalas VG, Zoval JV, et al. 2007. Centrifugal microfluidics with integrated sensing microdome optodes for multiion detection. *Anal. Chem.* 79:8046–54
8. Shortreed MR, Dourado S, Kopelman R. 1997. Development of a fluorescent optical potassium-selective ion sensor with ratiometric response for intracellular applications. *Sens. Actuators B* 38:8–12
9. Koronczi I, Reichert J, Heinzmann G, Ache HJ. 1998. Development of a submicron optochemical potassium sensor with enhanced stability due to internal reference. *Sens. Actuators B* 51:188–95
10. Brasuel M, Kopelman R, Miller TJ, Tjalkens R, Philbert MA. 2001. Fluorescent nanosensors for intracellular chemical analysis: decyl methacrylate liquid polymer matrix and ion-exchange-based potassium PEBBLE sensors with real-time application to viable rat C6 glioma cells. *Anal. Chem.* 73:2221–28
11. Totu E, Josceanu AM, Covington AK. 2001. Improved potassium-selective membrane using valinomycin as ionophore for ion-selective microdevices. *Mater. Sci. Eng. C* 18:87–91
12. Johnson RD, Badr IHA, Barrett G, Lai S, Lu Y, et al. 2001. Development of a fully integrated analysis system for ions based on ion-selective optodes and centrifugal microfluidics. *Anal. Chem.* 73:3940–46
13. Retter R, Peper S, Bell M, Tsagkatakis I, Bakker E. 2002. Flow cytometric ion detection with plasticized poly(vinyl chloride) microspheres containing selective ionophores. *Anal. Chem.* 74:5420–25
14. Xu C, Wygladacz K, Retter R, Bell M, Bakker E. 2007. Multiplexed flow cytometric sensing of blood electrolytes in physiological samples using fluorescent bulk optode microspheres. *Anal. Chem.* 79:9505–12

15. Wygladacz K, Bakker E. 2005. Imaging fiber microarray fluorescent ion sensors based on bulk optode microspheres. *Anal. Chim. Acta* 532:61–69
16. Xie L, Qin Y, Chen H-Y. 2013. Direct fluorescent measurement of blood potassium with polymeric optical sensors based on upconverting nanomaterials. *Anal. Chem.* 85:2617–22
17. O'Neill S, Conway S, Twellmeyer J, Egan O, Nolan K, Diamond D. 1999. Ion-selective optode membranes using 9-(4-diethylamino-2-octadecanoatestyryl)-acridine acidochromic dye. *Anal. Chim. Acta* 398:1–11
18. Tsagkatakis L, Peper S, Retter R, Bell M, Bakker E. 2001. Monodisperse plasticized poly(vinyl chloride) fluorescent microspheres for selective ionophore-based sensing and extraction. *Anal. Chem.* 73:6083–87
19. Xu C, Wygladacz K, Retter R, Bell M, Bakker E. 2007. Multiplexed flow cytometric sensing of blood electrolytes in physiological samples using fluorescent bulk optode microspheres. *Anal. Chem.* 79(24):9505–12
20. Wang E, Zhu L, Ma L, Patel H. 1997. Optical sensors for sodium, potassium and ammonium ions based on lipophilic fluorescein anionic dye and neutral carriers. *Anal. Chim. Acta* 357:85–90
21. Bychkova V, Shvarev A. 2009. Surface area effects on the response mechanism of ion optodes: a preliminary study. *Anal. Chem.* 81:7416–19
22. Seiler K, Wang K, Bakker E, Morf WE, Rusterholz B, et al. 1991. Characterization of sodium-selective optode membranes based on neutral ionophores and assay of sodium in plasma. *Clin. Chem.* 37(8):1350–55
23. Wang EJ, Meyerhoff ME. 1993. Anion-selective optical sensing with metalloporphyrin-doped polymeric films. *Anal. Chim. Acta* 283:673–82
24. Badr IHA, Johnson RD, Diaz M, Hawthorne MF, Bachas LG. 2000. A selective optical sensor based on [9]mercuracarborand-3, a new type of ionophore with a chloride complexing cavity. *Anal. Chem.* 72:4249–54
25. Pimenta AM, Araujo AN, Conceicao M, Montenegro BSM, Pasquini C, et al. 2004. Chloride-selective membrane electrodes and optodes based on an indium(III) porphyrin for the determination of chloride in a sequential injection analysis system. *J. Pharm. Biomed. Anal.* 36:49–55
26. Wygladacz K, Bakker E. 2005. Imaging fiber microarray fluorescent ion sensors based on bulk optode microspheres. *Anal. Chim. Acta* 532:61–69
27. Xu C, Qin Y, Bakker E. 2004. Optical chloride sensor based on [9]mercuracarborand-3 with massively expanded measuring range. *Talanta* 63:180–84
28. Tan SSS, Hauser PC, Wang KM, Fluri K, Seiler K, et al. 1991. Reversible optical sensing membrane for the determination of chloride in serum. *Anal. Chim. Acta* 255:35–44
29. Capitán-Vallvey LF, Arroyo-Guerrero E, Fernández-Ramos MD, Cuadros-Rodriguez L. 2006. Logit linearization of analytical response curves in optical disposable sensors based on coextraction for monovalent anions. *Anal. Chim. Acta* 561:156–63
30. Ceresa A, Qin Y, Peper S, Bakker E. 2003. Mechanistic insights into the development of optical chloride sensors based on the [9]mercuracarborand-3 ionophore. *Anal. Chem.* 75:133–40
31. Hisamoto H, Watanabe K, Oka H, Nakagawa E, Spichiger UE, Suzuki K. 1994. Flow-through type chloride ion selective optodes based on lipophilic organometallic chloride adducts and a lipophilic anionic dye. *Anal. Sci.* 10:615–22
32. Wang EJ, Ma L, Zhu L, Stivanello CM. 1997. Calcium optical sensors based on lipophilic anionic dye and calcium-selective organophosphate ionophore or neutral carrier. *Anal. Lett.* 30:33–44
33. Capel-Cuevas S, de Orbe-Paya I, Santoyo-Gonzalez F, Capitan-Vallvey LF. 2009. Double-armed crown ethers for calcium optical sensors. *Talanta* 78:1484–88
34. Hisamoto H, Yasuoka M, Terabe S. 2006. Integration of multiple-ion-sensing on a capillary-assembled microchip. *Anal. Chim. Acta* 556:164–70
35. Hisamoto H, Kim KH, Manabe Y, Sasaki K, Minamitani H, Suzuki K. 1997. Ion-sensitive and selective active waveguide optodes. *Anal. Chim. Acta* 342:31–39
36. Hisamoto H, Watanabe K, Nakagawa E, Siswanta D, Shichi Y, Suzuki K. 1994. Flow-through type calcium ion selective optodes based on novel neutral ionophores and a lipophilic anionic dye. *Anal. Chim. Acta* 299:179–87

37. Capitan-Vallvey LF, Fernandez-Ramos MD, Galvez PAD, Santoyo-Gonzalez F. 2003. Characterisation of a transparent optical test strip for quantification of water hardness. *Anal. Chim. Acta* 481:139–48
38. Qin Y, Mi YM, Bakker E. 2000. Determination of complex formation constants of 18 neutral alkali and alkaline earth metal ionophores in poly(vinyl chloride) sensing membranes plasticized with bis(2-ethylhexyl)sebacate and *o*-nitrophenyloctylether. *Anal. Chim. Acta* 421:207–20
39. Siswanta D, Hisamoto H, Sato S, Matsumoto Y, Koike Y, et al. 1997. Magnesium ion-selective optodes based on a neutral ionophore and a lipophilic cationic dye. *Anal. Sci.* 13:429–35
40. Lapresta-Fernández A, Capitán-Vallvey LF. 2011. Environmental monitoring using a conventional photographic digital camera for multianalyte disposable optical sensors. *Anal. Chim. Acta* 706:328–37
41. Wygladacz K, Qin Y, Wroblewski W, Bakker E. 2008. Phosphate-selective fluorescent sensing microspheres based on uranyl salophene ionophores. *Anal. Chim. Acta* 614:77–84
42. Xie X, Pawlak M, Tercier-Waeber M-L, Bakker E. 2012. Direct optical carbon dioxide sensing based on a polymeric film doped with a selective molecular tweezer-type ionophore. *Anal. Chem.* 84:3163–69
43. Shortreed MR, Barker SLR, Kopelman R. 1996. Anion-selective liquid-polymer optodes with fluorescent pH chromoionophores, tunable dynamic range and diffusion enhanced lifetimes. *Sens. Actuators B* 35:217–21
44. Badr IHA. 2001. Nitrite-selective optical sensors based on organopalladium ionophores. *Anal. Lett.* 34:2019–34
45. Capitán-Vallvey LF, Fernández Ramos MD, Al-Natsheh M. 2003. A disposable single-use optical sensor for potassium determination based on neutral ionophore. *Sens. Actuators B* 88:217–22
46. Hisamoto H, Miyashita N, Watanabe K, Nakagawa E, Yamamoto N, Suzuki K. 1995. Ion sensing film optodes: disposable ion sensing probes for the determination of Na^+, K^+, Ca^{2+} and Cl^- concentrations in serum. *Sens. Actuators B* 29:378–85
47. Lapresta-Fernández A, Huertas R, Melgosa M, Capitán-Vallvey LF. 2009. Colourimetric characterisation of disposable optical sensors from spectroradiometric measurements. *Anal. Bioanal. Chem.* 393:1361–66
48. He H, Jenkins K, Lin C. 2008. A fluorescent chemosensor for calcium with excellent storage stability in water. *Anal. Chim. Acta* 611:197–204
49. Chan WH, Yang RH, Mo T, Wang KM. 2002. Lead-selective fluorescent optode membrane based on 3,3′,5,5′-tetramethyl-*N*-(9-anthrylmethyl)benzidine. *Anal. Chim. Acta* 460:123–32
50. Antico E, Lerchi M, Rusterholz B, Achermann N, Badertscher M, et al. 1999. Monitoring Pb^{2+} with optical sensing films. *Anal. Chim. Acta* 388:327–38
51. Ceresa A, Pretsch E. 1999. Determination of formal complex formation constants of various Pb^{2+} ionophores in the sensor membrane phase. *Anal. Chim. Acta* 395:41–52
52. Bualom C, Ngeontae W, Nitiyanontakit S, Ngamukot P, Imyim A, et al. 2010. Bulk optode sensors for batch and flow-through determinations of lead ion in water samples. *Talanta* 82:660–67
53. Lerchi M, Bakker E, Rusterholz B, Simon W. 1992. Lead-selective bulk optodes based on neutral ionophores with subnanomolar detection limits. *Anal. Chem.* 64:1534–40
54. Ongun MZ, Ertekin K, Gocmenturk M, Ergun Y, Suslu A. 2012. Copper ion sensing with fluorescent electrospun nanofibers. *Spectrochim. Acta A* 90:177–85
55. Liu X, Qin Y. 2008. Ion-exchange reaction of silver(I) and copper(II) in optical sensors based on thiaglutaric diamide. *Anal. Sci.* 24:1151–56
56. Xie X, Li X, Ge Y, Qin Y, Chen H-Y. 2010. Rhodamine-based ratiometric fluorescent ion-selective bulk optodes. *Sens. Actuators B* 151:71–76
57. Firooz AR, Ensafi AA, Kazemifard N, Sharghi H. 2012. A highly sensitive and selective bulk optode based on benzimidazol derivative as an ionophore and ETH5294 for the determination of ultra trace amount of silver ions. *Talanta* 101:171–76
58. Hisamoto H, Nakagawa E, Nagatsuka K, Abe Y, Sato S, et al. 1995. Silver ion-selective optodes based on novel thia ether compounds. *Anal. Chem.* 67:1315–21
59. Wygladacz K, Radu A, Xu C, Qin Y, Bakker E. 2005. Fiber-optic microsensor array based on fluorescent bulk optode microspheres for the trace analysis of silver ions. *Anal. Chem.* 77:4706–12
60. Kuswandi B, Nuriman, Dam HH, Reinhoudt DN, Verboom W. 2007. Development of a disposable mercury ion-selective optode based on trityl-picolinamide as ionophore. *Anal. Chim. Acta* 591:208–13

61. Sadeghi S, Doosti S. 2008. Novel PVC membrane bulk optical sensor for determination of uranyl ion. *Sens. Actuators B* 135:139–44
62. Lerchi M, Reitter E, Simon W. 1994. Uranyl ion-selective optode based on neutral ionophores. *Fresenius J. Anal. Chem.* 348:272–76
63. Joshi JM, Pathak PN, Pandey AK, Manchanda VK. 2008. Optode for uranium(VI) determination in aqueous medium. *Talanta* 76:60–65
64. Puyol M, Salinas I, Garces I, Villuendas F, Llobera A, et al. 2002. Improved integrated waveguide absorbance optodes for ion-selective sensing. *Anal. Chem.* 74:3354–61
65. Bühlmann P, Pretsch E, Bakker E. 1998. Carrier-based ion-selective electrodes and bulk optodes. 2. Ionophores for potentiometric and optical sensors. *Chem. Rev.* 98:1593–688
66. Ozawa S, Hauser PC, Seiler K, Tan SSS, Morf WE, Simon W. 1991. Ammonia-gas-selective optical sensors based on neutral ionophores. *Anal. Chem.* 63(6):640–44
67. Seiler K, Wang K, Bakker E, Morf WE, Rusterholz B, et al. 1991. Characterization of sodium-selective optode membranes based on neutral ionophores and assay of sodium in plasma. *Clin. Chem.* 37(8):1350–55
68. Huber C, Werner T, Krause C, Wolfbeis OS, Leiner MJP. 1999. Overcoming the pH dependency of optical sensors: a pH-independent chloride sensor based on co-extraction. *Anal. Chim. Acta* 398:137–43
69. Krause C, Werner T, Huber C, Wolfbeis OS, Leiner MJ. 1999. pH-insensitive ion selective optode: a coextraction-based sensor for potassium ions. *Anal. Chem.* 71:1544–48
70. Krause C, Werner T, Huber C, Wolfbeis OS. 1999. Emulsion-based fluorosensors for potassium featuring improved stability and signal change. *Anal. Chem.* 71:5304–8
71. Charlton SC, Fleming RL, Zipp A. 1982. Solid-phase colorimetric determination of potassium. *Clin. Chem.* 28:1857–61
72. Ueberfeld J, Parthasarathy N, Zbinden H, Gisin N, Buffle J. 2002. Coupling fiber optics to a permeation liquid membrane for heavy metal sensor development. *Anal. Chem.* 74:664–70
73. Bakker E, Lerchi M, Rosatzin T, Rusterholz B, Simon W. 1993. Synthesis and characterization of neutral hydrogen ion-selective chromoionophores for use in bulk optodes. *Anal. Chim. Acta* 278:211–25
74. Bakker E, Bühlmann P, Pretsch E. 1997. Carrier-based ion-selective electrodes and bulk optodes. 1. General characteristics. *Chem. Rev.* 97:3083–132
75. Ishikawa J, Sakamoto H, Mizuno T, Doi K, Otomo M. 1998. Acyclic and cyclic polythiamonoaza- and polythiadiaza-alkane hydrazone derivatives as chromogenic extractants for silver ion. *Analyst* 123:201–7
76. Lan BTT, Toth K. 1998. Characterization of chromogenic calix[4]arene derivative based ion-selective optical sensors. *Anal. Sci.* 14:191–97
77. Sanchez-Pedreno C, Ortuno JA, Albero MI, Garcia MS, Valero MV. 2000. Development of a new bulk optode membrane for the determination of mercury(II). *Anal. Chim. Acta* 414:195–203
78. Kacmaz S, Ertekin K, Suslu A, Ozdemir M, Ergun Y, et al. 2011. Emission-based sub-nanomolar silver sensing with electrospun nanofibers. *Sens. Actuators B* 153:205–13
79. He HR, Mortellaro MA, Leiner MJP, Young ST, Fraatz RJ, Tusa JK. 2003. A fluorescent chemosensor for sodium based on photoinduced electron transfer. *Anal. Chem.* 75:549–55
80. Crespo GA, Bakker E. 2012. Ionophore-based ion optodes without a reference ion: electrogenerated chemiluminescence for potentiometric sensors. *Analyst* 137:4988–94
81. Crespo GA, Mistlberger G, Bakker E. 2012. Electrogenerated chemiluminescence for potentiometric sensors. *J. Am. Chem. Soc.* 134:205–7
82. Crespo GA, Mistlberger G, Bakker E. 2011. Electrogenerated chemiluminescence triggered by electroseparation of $Ru(bpy)_3^{2+}$ across a supported liquid membrane. *Chem. Commun.* 47:11644–46
83. Rosatzin T, Bakker E, Suzuki K, Simon W. 1993. Lipophilic and immobilized anionic additives in solvent polymeric membranes of cation-selective chemical sensors. *Anal. Chim. Acta* 280:197–208
84. Mistlberger G, Crespo GA, Xie X, Bakker E. 2012. Photodynamic ion sensor systems with spiropyran: photoactivated acidity changes in plasticized poly(vinyl chloride). *Chem. Commun.* 48:5662–64
85. Watanabe K, Nakagawa E, Yamada H, Hisamoto H, Suzuki K. 1993. Lithium ion-selective optical sensor-based on a novel neutral ionophore and a lipophilic anionic dye. *Anal. Chem.* 65:2704–10
86. Bakker E, Simon W. 1992. Selectivity of ion-sensitive bulk optodes. *Anal. Chem.* 64:1805–12

87. Lerchi M, Reitter E, Simon W, Pretsch E, Chowdhury DA, Kamata S. 1994. Bulk optodes based on neutral dithiocarbamate ionophores with high selectivity and sensitivity for silver and mercury cations. *Anal. Chem.* 66:1713–17
88. Puyol M, del Valle M, Garcés I, Villuendas F, Domínguez C, Alonso J. 1999. Integrated waveguide absorbance optode for chemical sensing. *Anal. Chem.* 71:5037–44
89. Kim K, Minamitani H. 2000. Active optical poly(vinylchloride) thin-film waveguide ion sensor. *Opt. Rev.* 7:152–57
90. Kovacs B, Nagy G, Dombi R, Toth K. 2003. Optical biosensor for urea with improved response time. *Biosens. Bioelectron.* 18:111–18
91. Kang Y, Kampf JW, Meyerhoff ME. 2007. Optical fluoride sensor based on monomer-dimer equilibrium of scandium(III)-octaethylporphyrin in a plasticized polymeric film. *Anal. Chim. Acta* 598:295–303
92. Clark PMS, Broughton PMG. 1983. An evaluation of the Ames Seralyzer. *J. Anal. Methods Chem.* 5:22–26
93. Walter B. 1983. Dry reagent chemistries in clinical analysis. *Anal. Chem.* 55:498A–514A
94. Palma AJ, Ortigosa JM, Lapresta-Fernández A, Fernández-Ramos MD, Carvajal MA, Capitán-Vallvey LF. 2008. Portable light-emitting diode-based photometer with one-shot optochemical sensors for measurement in the field. *Rev. Sci. Instrum.* 79:103105
95. Palma A, Lapresta-Fernández A, Ortigosa-Moreno JM, Fernández-Ramos MD, Carvajal MA, Capitán-Vallvey LF. 2006. A simplified measurement procedure and portable electronic photometer for disposable sensors based on ionophore-chromoionophore chemistry for potassium determination. *Anal. Bioanal. Chem.* 386:1215–24
96. Fernández-Ramos DM, Greluk M, Palma AJ, Arroyo-Guerrero E, Gomez-Sanchez J, Capitán-Vallvey LF. 2008. The use of one-shot sensors with a dedicated portable electronic radiometer for nitrate measurements in aqueous solutions. *Meas. Sci. Technol.* 19:095204
97. Prabhakaran D, Nanjo H, Matsunaga H. 2007. Naked eye sensor on polyvinyl chloride platform of chromo-ionophore molecular assemblies: a smart way for the colorimetric sensing of toxic metal ions. *Anal. Chim. Acta* 601:108–17
98. Garcia A, Erenas MM, Marinetto ED, Abad CA, de Orbe-Paya I, et al. 2011. Mobile phone platform as portable chemical analyzer. *Sens. Actuators B* 156:350–59
99. Lapresta-Fernández A, Capitán-Vallvey LF. 2011. Multi-ion detection by one-shot optical sensors using a colour digital photographic camera. *Analyst* 136:3917–26
100. Ye N, Wygladacz K, Bakker E. 2007. Absorbance characterization of microsphere-based ion-selective optodes. *Anal. Chim. Acta* 596:195–200
101. Xu C, Bakker E. 2007. Multicolor quantum dot encoding for polymeric particle-based optical ion sensors. *Anal. Chem.* 79:3716–23
102. Dubach JM, Harjes DI, Clark HA. 2007. Fluorescent ion-selective nanosensors for intracellular analysis with improved lifetime and size. *Nano. Lett.* 7:1827–31
103. Clark HA, Hoyer M, Philbert MA, Kopelman R. 1999. Optical nanosensors for chemical analysis inside single living cells. 1. Fabrication, characterization, and methods for intracellular delivery of pebble sensors. *Anal. Chem.* 71:4831–36
104. Roe JN, Szoka FC, Verkman AS. 1990. Fiber optic sensor for the detection of potassium using fluorescence energy transfer. *Analyst* 115:353–58
105. Wygladacz K, Bakker E. 2007. Fluorescent microsphere fiber optic microsensor array for direct iodide detection at low picomolar concentrations. *Analyst* 132:268–72
106. Xie L, Qin Y, Chen H-Y. 2012. Polymeric optodes based on upconverting nanorods for fluorescent measurements of pH and metal ions in blood samples. *Anal. Chem.* 84:1969–74
107. Freiner D, Kunz RE, Citterio D, Spichiger UE, Gale MT. 1995. Integrated optical sensors based on refractometry of ion-selective membranes. *Sens. Actuators B* 29:277–85
108. Kurihara K, Nakamura K, Hirayama E, Suzuki K. 2002. An absorption-based surface plasmon resonance sensor applied to sodium ion sensing based on an ion-selective optode membrane. *Anal. Chem.* 74:6323–33
109. Kurihara K, Ohkawa H, Iwasaki Y, Niwa O, Tobita T, Suzuki K. 2004. Fiber-optic conical microsensors for surface plasmon resonance using chemically etched single-mode fiber. *Anal. Chim. Acta* 523:165–70

110. Kurihara K, Ohtsu M, Yoshida T, Abe T, Hisamoto H, Suzuki K. 1999. Micrometer-sized sodium ion-selective optodes based on a "tailed" neutral ionophore. *Anal. Chem.* 71:3558–66
111. Spiess AC, Zavrel M, Ansorge-Schumacher MB, Janzen C, Michalik C, et al. 2008. Model discrimination for the propionic acid diffusion into hydrogel beads using lifetime confocal laser scanning microscopy. *Chem. Eng. Sci.* 63:3457–65
112. Kuwana E, Liang F, Sevick-Muraca EM. 2004. Fluorescence lifetime spectroscopy of a pH-sensitive dye encapsulated in hydrogel beads. *Biotechnol. Prog.* 20:1561–66
113. Huber C, Klimant I, Krause C, Wolfbeis OS. 2001. Dual lifetime referencing as applied to a chloride optical sensor. *Anal. Chem.* 73:2097–103
114. Tohda K, Gratzl M. 2006. Micro-miniature autonomous optical sensor array for monitoring ions and metabolites 1: design, fabrication, and data analysis. *Anal. Sci.* 22:383–88
115. Tohda K, Gratzl M. 2006. Micro-miniature autonomous optical sensor array for monitoring ions and metabolites 2: color responses to pH, K^+ and glucose. *Anal. Sci.* 22:937–41
116. Cantrell K, Erenas MM, de Orbe-Paya I, Capitán-Vallvey LF. 2010. Use of the hue parameter of the hue, saturation, value color space as a quantitative analytical parameter for bitonal optical sensors. *Anal. Chem.* 82:531–42
117. Xie X, Mistlberger G, Bakker E. 2012. Reversible photodynamic chloride-selective sensor based on photochromic spiropyran. *J. Am. Chem. Soc.* 134:16929–32
118. Mistlberger G, Xie X, Pawlak M, Crespo GA, Bakker E. 2013. Photoresponsive ion extraction/release systems: dynamic ion optodes for calcium and sodium based on photochromic spiropyran. *Anal. Chem.* 85:2983–90